
DEEP OPERATOR LEARNING LESSENS THE CURSE OF DIMENSIONALITY FOR PDES

Ke Chen

Department of Mathematics
University of Maryland College Park
College Park, MD, USA
kechen@umd.edu

Chunmei Wang

Department of Mathematics
University of Florida
Gainesville
chunmei.wang@ufl.edu

Haizhao Yang

Department of Mathematics
University of Maryland College Park
College Park, MD, USA
hzyang@umd.edu

ABSTRACT

Deep neural networks (DNNs) have seen tremendous success in many fields and their developments in PDE-related problems are rapidly growing. This paper provides an estimate for the generalization error of learning Lipschitz operators over Banach spaces using DNNs with applications to various PDE solution operators. The goal is to specify DNN width, depth, and the number of training samples needed to guarantee a certain testing error. Under mild assumptions on data distributions or operator structures, our analysis shows that deep operator learning can have a relaxed dependence on the discretization resolution of PDEs and, hence, lessen the curse of dimensionality in many PDE-related problems. We apply our results to various PDEs, including elliptic equations, parabolic equations, and Burgers equations.

1 Introduction

Nonlinear operator learning aims to learn a map from a parametric function space to the solution space of certain partial differential equation (PDE) problems. It has become an important topic for many fields with wide applications, including order reduction [1], parametric PDEs [2, 3], inverse problems [4], and imaging problems [5, 6, 7]. As deep neural networks (DNNs) become state-of-the-art models in various machine learning tasks [8, 9, 10], its tremendous success has drawn attention to their applications to engineering problems, where PDEs have been the dominating model for decades. Thus deep operator learning naturally arises as a powerful tool for nonlinear PDE operator learning [11, 3, 12, 4]. A typical method is to first discretize the computational domain and represents functions as a vector that tabulates the function values on the discretized mesh. Then the DNN is employed to learn a map between finite dimensional spaces. Although this method has been successful in many applications [13, 14], the computational cost is expensive due to the mesh-dependent nature of this method, that is, the DNN needs to be trained again if a different discretization is used. To tackle this issue, another line of works [15, 3, 16, 17] are proposed for problems with sparsity structures with discretization-invariant property.

Despite the empirical success of deep operator learning in many applications, the statistical learning theory is very limited, especially when the ambient space is infinite-dimensional. Generally speaking, the learning theory consists of three parts: the approximation theory that quantifies the expressibility of various DNNs as a surrogate for a class of operators, the optimization theory that analyzes various optimization schemes and non-convexity nature of the optimization task, and the generalization theory that assesses the discrepancy when only finite many training data is available. The approximation theory of DNNs originates from the universal approximation theory for a certain class of functions [18, 19], and then was extended to other classes of functions such as continuous function [20, 21, 22], certain smooth functions [23, 24, 25], and functions with integral representations [26, 27]. In comparison to many theoretic works in approximation theory for high dimensional functions, the approximation theory for operators, especially between infinite dimensional spaces, are however very limited. Seminal quantitative results were given in [28, 11].

The generalization theory aims to answer the following question:

How many training samples are needed if one wants to achieve a certain testing error?

This question has been answered by many statistical learning theory works for function regression via neural network structures [29, 30, 31, 32, 33, 34, 35]. A typical error decay rate in a d -dimensional learning problem is at the order of $n^{-\mathcal{O}(1/d)}$ when the number of samples n grows. The fact that the exponent is very small for large dimensionality d is called the *curse of dimensionality* (CoD) [36]. It is shown that DNNs can achieve a faster decay rate when the target function or the domain of the function has a low dimensional structure [37, 30, 38, 34, 39, 20]. The decay rate can be made independent of the domain discretization, thus the CoD is lessened [29, 40, 25]. However, most works are only focusing on functions between finite dimensional spaces. To the best of our knowledge, the works [41, 11, 2, 42] are the only generalization analysis for infinite dimensional functions. Our work generalizes the result in [42] to Banach spaces with new analyses in PDE problems. The removal of the inner-product assumption is crucial for applying the estimate for various PDE problems as most PDE regularity results are built for Banach spaces such as L^p space and continuous functions C^k .

1.1 Our contributions

The main goal of this work is to investigate why deep operator learning lessens the CoD for PDE-related problems. The key observation is that most PDE operators admit a structure of compositions of linear transformations and entrywise nonlinear transformations of few inputs. Such a structure can be efficiently learned by DNNs due to its pointwise network evaluation nature. We provide an error analysis of the approximation and generalization errors, and apply it to various PDE problems to reveal to what extent can the CoD be mitigated. We summarize our contributions as follows:

- We derive approximation and generalization error estimates for general PDE operators that are Lipschitz continuous in the Banach spaces. To the best of our knowledge, this is the first error analysis for PDE operator learning beyond Hilbert spaces.
- We combine the regularity estimates of various PDE operators with our DNN error estimates, leading to explicit sample complexity and DNN size estimates for different PDE solution operators with typical PDE discretization such as the spectral methods. Our method can be easily generalized with ease for other discretization types. This leads to an explicit estimate of the number of samples and the DNN size needed to achieve a certain testing error.
- Under mild assumptions, we are able to make our estimate independent of the PDE discretization size. This leads to a sample complexity and DNN size that only depends on the *essential dimension* of the PDE itself, rather than the PDE discretion size, which explains why deep operator learning mitigates CoD.

2 Problem setup and main results

Notations. For a general Banach space \mathcal{X} , we denote its endowed norm by $\|\cdot\|_{\mathcal{X}}$. We also denote by $E_{\mathcal{X}}^n$ the encoder from a Banach space \mathcal{X} to a Euclidean space $\mathbb{E}^{d_{\mathcal{X}}}$ where $d_{\mathcal{X}}$ is the dimension. We denote the decoder for \mathcal{X} by $D_{\mathcal{X}}^n$ analogously.

2.1 Operator learning and loss functions

We consider a general PDE operator $\Phi : \mathcal{X} \ni u \mapsto v \in \mathcal{Y}$ over Banach spaces \mathcal{X} and \mathcal{Y} . The input variable u usually stands for the initial condition, boundary condition, and the source of a certain PDE, while the output variable v usually represents the PDE solution or partial measurements of the solution. Our goal is to train a DNN $\phi(u; \theta)$ to approximate the target operator Φ with a given data set $\mathcal{S} = \{(u_i, v_i), v_i = \Phi(u_i) + \varepsilon_i, i = 1, \dots, 2n\}$. Here the inputs of both training data S_1^n and S_2^n are generated i.i.d. from a random measure γ over \mathcal{X} with ε_i being the random noise. The data set \mathcal{S} is divided into a training data set $\mathcal{S}_1^n = \{(u_i, v_i), v_i = \Phi(u_i) + \varepsilon_i, i = 1, \dots, n\}$ and a testing data set $\mathcal{S}_2^n = \{(u_i, v_i), v_i = \Phi(u_i) + \varepsilon_i, i = n + 1, \dots, 2n\}$.

In practice, DNNs are implemented over finite-dimensional spaces. Therefore, an empirical encoder-decoder pair, $E_{\mathcal{X}}^n : \mathcal{X} \rightarrow \mathbb{R}^{d_{\mathcal{X}}}$ and $E_{\mathcal{Y}}^n : \mathcal{Y} \rightarrow \mathbb{R}^{d_{\mathcal{Y}}}$, is applied to discretize $u \in \mathcal{X}$. Similarly, an empirical encoder-decoder pair, $D_{\mathcal{X}}^n : \mathbb{R}^{d_{\mathcal{X}}} \rightarrow \mathcal{X}$ and $D_{\mathcal{Y}}^n : \mathbb{R}^{d_{\mathcal{Y}}} \rightarrow \mathcal{Y}$, is used for $v \in \mathcal{Y}$. These encoder-decoder pairs are either trained with the available data set \mathcal{S}_1^n or manually determined such that $D_{\mathcal{X}} \circ E_{\mathcal{X}} \approx \mathbb{I}_{\mathbb{R}^{d_{\mathcal{X}}}}$ and $D_{\mathcal{Y}} \circ E_{\mathcal{Y}} \approx \mathbb{I}_{\mathbb{R}^{d_{\mathcal{Y}}}}$. A typical example of empirical encoders and decoders is the discretization operator that projects a function to a vector that tabulates the function values over mesh points. Other examples are finite element projections and spectral methods that map functions to the coefficients of the corresponding basis functions. We aim to approximate the PDE operator via a finite-dimensional operator Γ so that $\Phi \approx D_{\mathcal{Y}}^n \circ \Gamma \circ E_{\mathcal{X}}^n$. See Figure 1. This is done by solving the following optimization

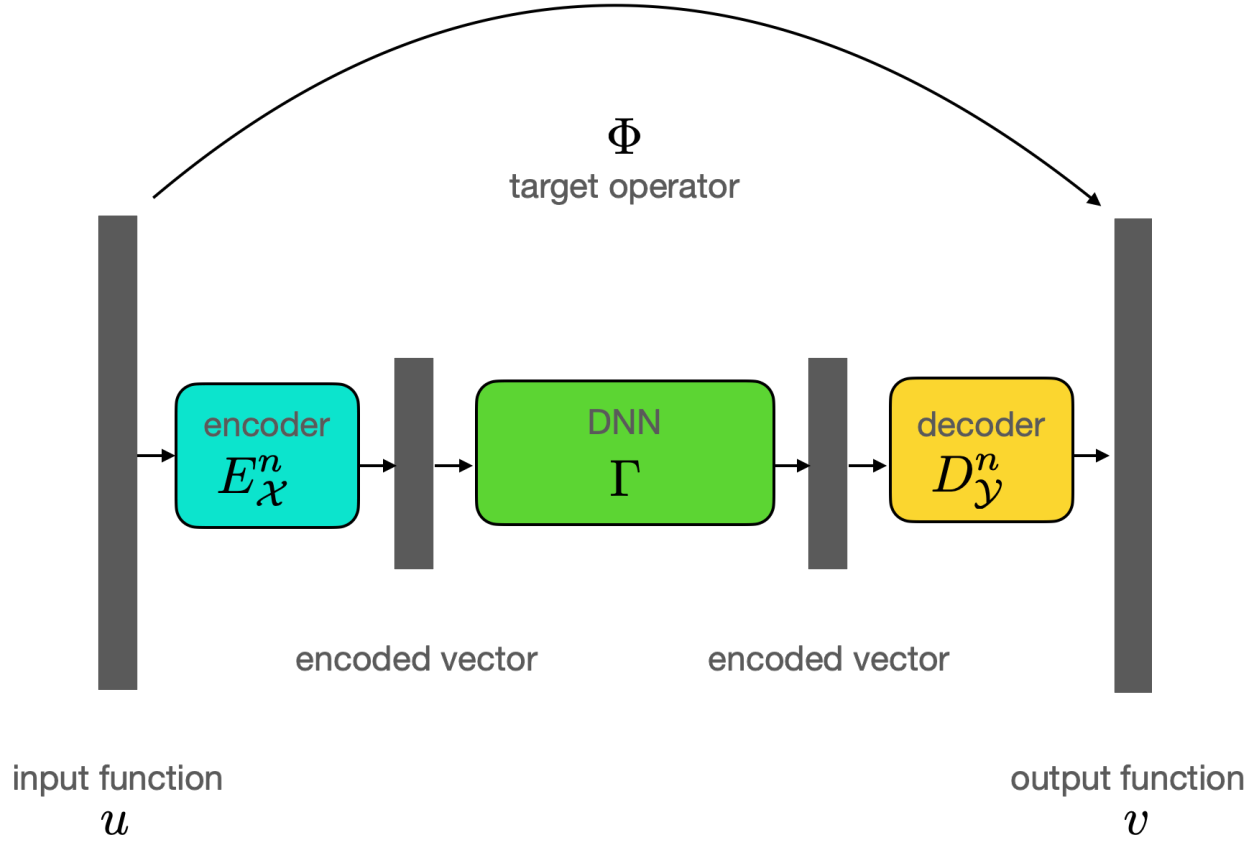


Figure 1: The target operator $\Phi : u \mapsto v$ is approximated by compositions of an encoder E_{χ}^n , a DNN function Γ , and a decoder D_{γ}^n . The finite dimensional operator Γ is learned via the optimization problem (2.1).

problem

$$\Gamma_{\text{NN}} \in \operatorname{argmin}_{\Gamma \in \mathcal{F}_{\text{NN}}} \frac{1}{n} \sum_{i=1}^n \|\Gamma \circ E_{\chi}^n(u_i) - E_{\gamma}^n(v_i)\|_2^2. \quad (2.1)$$

Here the function space \mathcal{F}_{NN} is a set of ReLU feedforward DNNs $f(x)$ defined as follows

$$f(x) = W_L \cdot \phi(W_{L-1} \cdots \phi(W_1 x + b_1) + \cdots + b_{L-1}) + b_L, \quad (2.2)$$

where W_i and b_i are the weight matrices and vectors respectively, and $\phi(x) = \max\{x, 0\}$ is called the rectified linear unit (ReLU) activation function. In practice, the functional space \mathcal{F}_{NN} is chosen as a compact set of all ReLU feedforward DNNs. Two different architectures of \mathcal{F}_{NN} are considered in this work. The first architecture is defined by

$$\begin{aligned} \mathcal{F}_{\text{NN}}(d, L, p, K, \kappa, M) = \{ & \Gamma = [f_1, f_2, \dots, f_d]^{\top} : \\ & \text{for each } k = 1, \dots, d, f_k(x) \text{ is in the form of (2.2)} \\ & \text{with } L \text{ layers, width bounded by } p, \\ & \|f_k\|_{\infty} \leq M, \|W_l\|_{\infty, \infty} \leq \kappa, \\ & \|b_l\|_{\infty} \leq \kappa, \sum_{l=1}^L \|W_l\|_0 + \|b_l\|_0 \leq K \}, \end{aligned} \quad (2.3)$$

where $\|f\|_{\infty} = \sup_x |f(x)|$, $\|W\|_{\infty, \infty} = \max_{i,j} |W_{i,j}|$, $\|b\|_{\infty} = \max_i |b_i|$ for any function f , matrix W , and vector b with $\|\cdot\|_0$ denoting the number of nonzero elements of its argument. By definition, the functions in this class have all parameters bounded by uniform constants with limited cardinalities. Such assumptions are dropped in the second

architecture, which thus has fewer constraints:

$$\begin{aligned} \mathcal{F}_{\text{NN}}(d, L, p, M) = \{ & \Gamma = [f_1, f_2, \dots, f_d]^\top : \\ & \text{for each } k = 1, \dots, d_{\mathcal{Y}}, f_k(x) \text{ is in the form of (2.2)} \\ & \text{with } L \text{ layers, width bounded by } p, \\ & \|f_k\|_\infty \leq M \}. \end{aligned} \quad (2.4)$$

We consider the following assumptions in our theories.

Assumption 2.1 (Compactly supported measure). The probability measure γ is supported on a compact set $\Omega_X \subset \mathcal{X}$. There exists $R_{\mathcal{X}} > 0$ such that for all $u \in \Omega_X$,

$$\|u\|_{\mathcal{X}} \leq R_{\mathcal{X}}.$$

Assumption 2.2 (Lipschitz operator). There exists $L_\Phi > 0$ such that

$$\|\Phi(u_1) - \Phi(u_2)\|_{\mathcal{Y}} \leq L_\Phi \|u_1 - u_2\|_{\mathcal{X}}, \text{ for any } u_1, u_2 \in \Omega_X.$$

Remark 2.3. The Lipschitz constant will be explicitly computed in Section 3 for different PDE operators.

Assumption 2.4 (Lipschitz encodes and decoders). The empirical encoders and decoders $E_{\mathcal{X}}^n, D_{\mathcal{X}}^n, E_{\mathcal{Y}}^n, D_{\mathcal{Y}}^n$ satisfy:

$$E_{\mathcal{X}}^n(0_{\mathcal{X}}) = \mathbf{0}, D_{\mathcal{X}}^n(\mathbf{0}) = 0_{\mathcal{X}}, E_{\mathcal{Y}}^n(0_{\mathcal{Y}}) = \mathbf{0}, D_{\mathcal{Y}}^n(\mathbf{0}) = 0_{\mathcal{Y}},$$

where $\mathbf{0}$ denotes the zero vector and $0_{\mathcal{X}}, 0_{\mathcal{Y}}$ denote the zero function in \mathcal{X} and \mathcal{Y} , respectively.

Assumption 2.5 (Noise). The noise $\tilde{\varepsilon} := [\varepsilon_i]_{i=1}^{2n}$ satisfies

1. $\tilde{\varepsilon}$ is independent of $u_i, i = 1, \dots, 2n$.
2. $\mathbf{E}[\tilde{\varepsilon}] = 0$.
3. There exists $\tilde{\sigma} > 0$ such that $\|\tilde{\varepsilon}\|_{\mathcal{Y}} \leq \tilde{\sigma}$.

Assumption 2.6 (Noise and encoder). For any noise satisfying Assumption 2.5 and any given data set \mathcal{S} , the conditional expectation satisfies that for any $u \in \Omega_X$,

$$\mathbf{E}_{\tilde{\varepsilon}} [E_{\mathcal{Y}}^n(\Phi(u) + \tilde{\varepsilon}) - E_{\mathcal{Y}}^n(\Phi(u)) \mid \mathcal{S}] = \mathbf{0},$$

where $E_{\mathcal{Y}}^n$ is the empirical encoder computed with \mathcal{S} .

2.2 Main Results

Theorem 2.7. Suppose Assumption 2.1 to Assumption 2.5 hold. Let Γ_{NN} be the minimizer of the optimization problem (2.1), with the network architecture $\mathcal{F}(d_{\mathcal{Y}}, L, p, K, \kappa, M)$ defined in (2.3) with parameters

$$\begin{aligned} L &= \mathcal{O}(d_{\mathcal{X}} \ln(\frac{n}{d_{\mathcal{Y}}}) + d_{\mathcal{X}} \ln(BR) + d_{\mathcal{X}}^2), \\ p &= \mathcal{O}(d_{\mathcal{Y}}^{\frac{-d_{\mathcal{X}}}{2+d_{\mathcal{X}}}} n^{\frac{d_{\mathcal{X}}}{2+d_{\mathcal{X}}}} 2^{d_{\mathcal{X}}^2}), \\ K &= \mathcal{O}(pL), \quad \kappa = \mathcal{O}(M^2), \quad M = \mathcal{O}(d_{\mathcal{X}} BR), \end{aligned}$$

There holds

$$\begin{aligned} & \mathbb{E}_{\mathcal{S}} \mathbb{E}_{u \sim \gamma} [\|D_{\mathcal{Y}}^n \circ \Gamma_{\text{NN}} \circ E_{\mathcal{X}}^n(u) - \Phi(u)\|_{\mathcal{Y}}^2] \\ & \lesssim d_{\mathcal{Y}}^{\frac{4+d_{\mathcal{X}}}{2+d_{\mathcal{X}}}} n^{-\frac{2}{2+d_{\mathcal{X}}}} L_{E_{\mathcal{Y}}^n}^2 R_{E_{\mathcal{Y}}^n}^2 2^{d_{\mathcal{X}}^2} (\ln^3 \frac{n}{d_{\mathcal{Y}}} + \ln^3(BR) + \ln^2 n) \\ & + L_{E_{\mathcal{Y}}^n}^2 L_{\Phi}^2 \mathbb{E}_u [\|\Pi_{\mathcal{X}, d_{\mathcal{X}}}^n(u) - u\|_{\mathcal{Y}}^2] \\ & + \mathbb{E}_{\mathcal{S}} \mathbb{E}_{w \sim \Phi_{\#} \gamma} [\|\Pi_{\mathcal{Y}, d_{\mathcal{Y}}}^n(w) - w\|_{\mathcal{Y}}^2] \\ & + L_{E_{\mathcal{Y}}^n}^2 \tilde{\sigma}^2 + n^{-1}, \end{aligned}$$

where all universal constants have been absorbed in \lesssim .

Theorem 2.8. Suppose Assumption 2.1 to Assumption 2.5 hold. Let Γ_{NN} be the minimizer of the optimization problem (2.1) with the network architecture $\mathcal{F}_{\text{NN}}(d_{\mathcal{Y}}, L, p, M)$ defined in (2.4) with parameters,

$$M = \sqrt{d_{\mathcal{Y}}} L_{E_{\mathcal{Y}}^n} R_{\mathcal{Y}}, \text{ and } Lp = \left[d_{\mathcal{Y}}^{-\frac{d_{\mathcal{X}}}{4+2d_{\mathcal{X}}}} n^{\frac{d_{\mathcal{X}}}{4+2d_{\mathcal{X}}}} \right]. \quad (2.5)$$

Then we have

$$\begin{aligned}
 & \mathbb{E}_{\mathcal{S}} \mathbb{E}_u \|D_{\mathcal{Y}}^n \circ \Gamma_{\text{NN}} \circ E_{\mathcal{X}}^n(u) - \Psi(u)\|_{\mathcal{Y}}^2 \\
 & \lesssim L_{\Phi}^2 d_{\mathcal{Y}}^{\frac{4+d_{\mathcal{X}}}{2+d_{\mathcal{X}}}} n^{-\frac{2}{2+d_{\mathcal{X}}}} \log^6 n + (\sigma^2 + n^{-1}) \\
 & + L_{\Phi}^2 \mathbb{E}_u [\|\Pi_{\mathcal{X}, d_{\mathcal{X}}}^n(u) - u\|_{\mathcal{Y}}^2] \\
 & + \mathbb{E}_{\mathcal{S}} \mathbb{E}_{w \sim \Phi_{\# \gamma}} [\|\Pi_{\mathcal{Y}, d_{\mathcal{Y}}}^n(w) - w\|_{\mathcal{Y}}^2],
 \end{aligned} \tag{2.6}$$

where \lesssim contains constants that depend on $d_{\mathcal{X}}, L_{E_{\mathcal{Y}}^n}, L_{E_{\mathcal{X}}^n}, L_{D_{\mathcal{Y}}^n}$ and $L_{D_{\mathcal{X}}^n}$.

Remark 2.9. The above results reveal that, with an appropriate choice of DNN width and depth, the generalization error can be decomposed into the generalization error of learning the finite-dimensional operator Γ , the projection error of the encoders/decoders, and the noise. The generalization error decays exponentially as the number of samples n grows. The presence of $d_{\mathcal{X}}$ in the exponent of sample complexity n indicates the CoD and might be pessimistic at the first glance, but we will show that it can be removed when the input data $\Omega_{\mathcal{X}}$ of the target operator has a low-dimensional data structure or the target operator itself has a low-complexity structure. These assumptions are usually satisfied for certain PDE operators with appropriate encoders.

Estimates with special data and operator structures

The generalization error estimates in Theorems 2.7 and 2.8 work well when the input dimension $d_{\mathcal{X}}$ is not large. However, in practice, numerous bases might be needed to reduce the encoder/decoder projection error in the estimate, which makes $d_{\mathcal{X}}$ a large number. Thus, the decay rate of generalization error in Theorem 2.7 and 2.8 is stagnant due to the exponential dependence on $d_{\mathcal{X}}$.

Nevertheless, it is often assumed that the high-dimensional data lie within the vicinity of a low-dimensional manifold by the famous ‘‘manifold hypothesis’’. Specifically, we assume that the encoded vectors u lie on a d_0 -dimensional manifold with $d_0 \ll d_{\mathcal{X}}$. Such a data distribution has been observed in many applications, including PDE solution set, manifold learning, and image recognition. We formulate this assumption in the following.

Assumption 2.10. Let $d_0 < d_{\mathcal{X}} \in \mathbb{N}$. Suppose there exists an encoder $E_{\mathcal{X}} : \mathcal{X} \rightarrow \mathbb{R}^{d_{\mathcal{X}}}$ such that $\{E_{\mathcal{X}}(u) \mid u \in \Omega_{\mathcal{X}}\}$ lies in a smooth d_0 -dimensional Riemannian manifold \mathcal{M} that is isometrically embedded in $\mathbb{R}^{d_{\mathcal{X}}}$. The reach [43] of \mathcal{M} is $\tau > 0$.

Under Assumption 2.10, the input data set has a low intrinsic dimension, which is not necessarily true for the noise-perturbed output data set though. In this section, we show that the DNN automatically adapts to the low-dimensional feature of the data set, so that the network estimation error only depends on the intrinsic dimension d_0 , instead of the large ambient dimension $d_{\mathcal{X}}$. In particular, we have the following result.

Theorem 2.11. Suppose Assumption 2.1 to Assumption 2.5, and Assumption 2.10 are true, let Γ_{NN} be the minimizer of the optimization problem (2.1) with the network architecture $\mathcal{F}_{\text{NN}}(d_{\mathcal{Y}}, L, p, M)$ defined in (2.4) with parameters

$$\begin{aligned}
 L &= O(\tilde{L} \log \tilde{L}), p = O(d_{\mathcal{X}} \tilde{p} \log \tilde{p}), \\
 M &= \sqrt{d_{\mathcal{Y}}} L_{E_{\mathcal{Y}}^n} R_{\mathcal{Y}},
 \end{aligned} \tag{2.7}$$

where $\tilde{L}, \tilde{p} > 0$ are integers such that $\tilde{L}\tilde{p} = \lceil \epsilon_1^{-d_0/2} \rceil$. Then we have

$$\begin{aligned}
 & \mathbb{E}_{\mathcal{S}} \mathbb{E}_u \|D_{\mathcal{Y}}^n \circ \Gamma_{\text{NN}} \circ E_{\mathcal{X}}^n(u) - \Psi(u)\|_{\mathcal{Y}}^2 \\
 & \lesssim L_{\Phi}^2 d_{\mathcal{Y}}^{\frac{4+d_0}{2+d_0}} n^{-\frac{2}{2+d_0}} \log^6 n + (\sigma^2 + n^{-1}) \\
 & + L_{\Phi}^2 \mathbb{E}_u [\|\Pi_{\mathcal{X}, d_{\mathcal{X}}}^n(u) - u\|_{\mathcal{Y}}^2] \\
 & + \mathbb{E}_{\mathcal{S}} \mathbb{E}_{w \sim \Phi_{\# \gamma}} [\|\Pi_{\mathcal{Y}, d_{\mathcal{Y}}}^n(w) - w\|_{\mathcal{Y}}^2],
 \end{aligned} \tag{2.8}$$

where the constants in \lesssim and $\mathcal{O}(\cdot)$ only depend on $d_0, \log d_{\mathcal{X}}, R_{\mathcal{X}}, R_{\mathcal{Y}}, L_{E_{\mathcal{X}}^n}, L_{E_{\mathcal{Y}}^n}, L_{D_{\mathcal{X}}^n}, L_{D_{\mathcal{Y}}^n}, \tau$, the surface area of \mathcal{M} .

Notice that the estimate (2.8) only has an algebraic dependence on $d_{\mathcal{X}}$ and $d_{\mathcal{Y}}$. The decay rate with respect to the sample size is no longer dependent on the ambient input dimension $d_{\mathcal{X}}$. Therefore, our results reveal that the CoD can be lessened via ‘‘manifold hypothesis’’. The width of the DNN has to be at the order of $O(d_{\mathcal{X}})$ to adapt to the data on a low-dimensional manifold. Another special structure that often presents in PDE problems is the low complexity of the target operator. This is often true when the target operator consists of several alternating compositions of a few linear transforms and nonlinear transforms with only few inputs. We quantify the concept of low-complexity operators in the following context.

Assumption 2.12. Consider an integer $0 < d_0 \leq d_{\mathcal{X}}$, and assume there exists $E_{\mathcal{X}}, D_{\mathcal{X}}, E_{\mathcal{Y}}, D_{\mathcal{Y}}$ such that for any $u \in \Omega_{\mathcal{X}}$, we have

$$\Pi_{\mathcal{Y}, d_{\mathcal{Y}}} \circ \Psi(u) = D_{\mathcal{Y}} \circ g \circ E_{\mathcal{X}}(u)$$

where $g : \mathbb{R}^{d_{\mathcal{X}}} \rightarrow \mathbb{R}^{d_{\mathcal{Y}}}$ is defined as

$$g(a) = [g_1(V_1^{\top} a), \dots, g_{d_{\mathcal{Y}}}(V_{d_{\mathcal{Y}}}^{\top} a)] ,$$

for some matrices $V_k \in \mathbb{R}^{d_{\mathcal{X}} \times d_0}$ and real valued functions $g_k : \mathbb{R}^{d_0} \rightarrow \mathbb{R}$ for $k = 1, \dots, d_{\mathcal{Y}}$.

In Assumption 2.12, when $d_0 = 1$ and $g_1 = \dots = g_{d_{\mathcal{Y}}}$, $g(a)$ is the composition of a pointwise nonlinear transform and a linear transform on a .

Theorem 2.13. Suppose Assumption 2.1 to Assumption 2.5, and Assumption 2.12 are true, let Γ_{NN} be the minimizer of the optimization problem (2.1) with the network architecture $\mathcal{F}_{\text{NN}}(d_{\mathcal{Y}}, L, p, M)$ defined in (2.4) with parameters

$$L = O\left(\tilde{L} \log \tilde{L}\right), p = O(\tilde{p} \log \tilde{p}), M = \sqrt{d_{\mathcal{Y}}} L_{E_{\mathcal{Y}}} R_{\mathcal{Y}},$$

where $\tilde{L}, \tilde{p} > 0$ are integers such that $\tilde{L}\tilde{p} = \left\lceil \epsilon_1^{-d_0/2} \right\rceil$. Then we have

$$\begin{aligned} & \mathbb{E}_{\mathcal{S}} \mathbb{E}_u \|D_{\mathcal{Y}}^n \circ \Gamma_{\text{NN}} \circ E_{\mathcal{X}}^n(u) - \Psi(u)\|_{\mathcal{Y}}^2 \\ & \lesssim L_{\Phi}^2 d_{\mathcal{Y}}^{\frac{4+d_0}{2+d_0}} n^{-\frac{2}{2+d_0}} \log^6 n + (\sigma^2 + n^{-1}) \\ & + L_{\Phi}^2 \mathbb{E}_u [\|\Pi_{\mathcal{X}, d_{\mathcal{X}}}^n(u) - u\|_{\mathcal{Y}}^2] \\ & + \mathbb{E}_{\mathcal{S}} \mathbb{E}_{w \sim \Phi_{\# \gamma}} [\|\Pi_{\mathcal{Y}, d_{\mathcal{Y}}}^n(w) - w\|_{\mathcal{Y}}^2], \end{aligned} \quad (2.9)$$

where the constants in \lesssim and $O(\cdot)$ only depend on $d_0, \log d_{\mathcal{X}}, R_{\mathcal{X}}, R_{\mathcal{Y}}, L_{E_{\mathcal{X}}}, L_{E_{\mathcal{Y}}}, L_{D_{\mathcal{X}}}, L_{D_{\mathcal{Y}}}$.

Remark 2.14. Under Assumption 2.12, our result indicates that the CoD can be mitigated to a cost $\mathcal{O}(n^{\frac{-2}{2+d_0}})$ because the main task of DNNs is to learn the nonlinear transforms $g_1, \dots, g_{d_{\mathcal{Y}}}$, which are functions over \mathbb{R}^{d_0} .

In practice, a PDE operator might be the repeated composition of operators in Assumption 2.12, which motivates a more general low-complexity assumption below.

Assumption 2.15. Considering integers $0 < d_1, \dots, d_k \leq d_{\mathcal{X}}$ and $0 < l_0, \dots, l_k \leq \min\{d_{\mathcal{X}}, d_{\mathcal{Y}}\}$ with $l_0 = d_{\mathcal{X}}$ and $l_k = d_{\mathcal{Y}}$, and assume there exists $E_{\mathcal{X}}, D_{\mathcal{X}}, E_{\mathcal{Y}}, D_{\mathcal{Y}}$ such that for any $u \in \Omega_{\mathcal{X}}$, we have

$$\Pi_{\mathcal{Y}, d_{\mathcal{Y}}} \circ \Psi(u) = D_{\mathcal{Y}} \circ G^k \circ \dots \circ G^1 \circ E_{\mathcal{X}}(u),$$

where $G^i : \mathbb{R}^{l_{i-1}} \rightarrow \mathbb{R}^{l_i}$ is defined as

$$G^i(a) = [g_1^i((V_1^i)^{\top} a), \dots, g_{l_i}^i((V_{l_i}^i)^{\top} a)] ,$$

for some matrices $V_j^i \in \mathbb{R}^{d_i \times l_{i-1}}$ and real valued functions $g_j^i : \mathbb{R}^{d_i} \rightarrow \mathbb{R}$ for $j = 1, \dots, l_i, i = 1, \dots, k$.

Theorem 2.16. Suppose Assumption 2.1 to Assumption 2.5, and Assumption 2.15 are true, let Γ_{NN} be the minimizer of the optimization problem (2.1) with the network architecture $\mathcal{F}_{\text{NN}}(d_{\mathcal{Y}}, L, p, M)$ defined in (2.4) with parameters

$$L = O\left(\tilde{L} \log \tilde{L}\right), p = O(\tilde{p} \log \tilde{p}), M = \sqrt{d_{\mathcal{Y}}} L_{E_{\mathcal{Y}}} R_{\mathcal{Y}},$$

where $\tilde{L}, \tilde{p} > 0$ are integers such that $\tilde{L}\tilde{p} = \left\lceil \epsilon_1^{-d_{\max}/2} \right\rceil$ with $d_{\max} = \max\{d_i\}_{i=1}^k$. Then we have

$$\begin{aligned} & \mathbb{E}_{\mathcal{S}} \mathbb{E}_u \|D_{\mathcal{Y}}^n \circ \Gamma_{\text{NN}} \circ E_{\mathcal{X}}^n(u) - \Psi(u)\|_{\mathcal{Y}}^2 \\ & \lesssim L_{\Phi}^2 l_{\max}^{\frac{4+d_{\max}}{2+d_{\max}}} n^{-\frac{2}{2+d_{\max}}} \log^6 n + (\sigma^2 + n^{-1}) \\ & + L_{\Phi}^2 \mathbb{E}_u [\|\Pi_{\mathcal{X}, d_{\mathcal{X}}}^n(u) - u\|_{\mathcal{Y}}^2] \\ & + \mathbb{E}_{\mathcal{S}} \mathbb{E}_{w \sim \Phi_{\# \gamma}} [\|\Pi_{\mathcal{Y}, d_{\mathcal{Y}}}^n(w) - w\|_{\mathcal{Y}}^2], \end{aligned}$$

where the constants in \lesssim and $O(\cdot)$ only depend on $k, d_{\max}, l_{\max}, R_{\mathcal{X}}, R_{\mathcal{Y}}, L_{E_{\mathcal{X}}}, L_{E_{\mathcal{Y}}}, L_{D_{\mathcal{X}}}, L_{D_{\mathcal{Y}}}$.

As we shall see later, many operators in PDE problems are the composition of low-complexity operators in Assumption 2.12 or Assumption 2.15. Therefore, deep operator learning can lessen the curse of dimensionality according to Theorem 2.13 or its generalized version in Theorem 2.16.

3 Explicit complexity bounds for various PDE operator learning

In practice, the uniform bound constraint in architecture (2.3) is usually not convenient to enforce and instead, the architecture (2.4) is implemented. To this end, we only consider the architecture (2.4) in this section. We assume all assumptions in Theorem 2.11 are satisfied in this section. Furthermore, we assume a Hölder regularity of the input space so that a simple encoder such as the spectral method can be applied. The Hölder function space C^s consists of functions with bounded Hölder norm, defined as the following

$$\|f\|_{C^s} = \|f\|_{C^k} + \max_{\beta=k} |D^\beta f|_{C^{0,\alpha}},$$

where $s = k + \alpha$, k is an integer, $0 < \alpha < 1$ and $|\cdot|_{C^{0,\alpha}}$ is the α -Hölder semi-norm

$$|f|_{C^{0,\alpha}} = \sup_{x \neq y} \frac{|f(x) - f(y)|}{\|x - y\|^\alpha}.$$

Similar analyses can be derived for other regularity assumptions if appropriate encoders/decoders are used.

First we analyze the L^p learning error of the spectral methods used as the encoder/decoder. In particular, a function $u \in \mathcal{X}$ is projected into the space P_d^r of the product of univariate polynomials with a degree less than r . The input dimension is thus $d_{\mathcal{X}} = \dim P_d^r = r^d$. Without loss of generality, we assume the computational domain is $[-1, 1]^d$. Our goal is to derive an upper bound of the projection error for functions with Hölder continuity. We will need the following lemma to achieve this.

Lemma 3.1 (Lemma 13 of [42]). *For any $f \in C^s([-1, 1]^d)$ with $s = k + \alpha$, $k \geq 0$ an integer and $0 < \alpha < 1$, denote its spectral approximation as \tilde{f} , then*

$$\|f - \tilde{f}\|_\infty \leq C_d \|f\|_{C^s} r^{-s},$$

where $s = k + \alpha$.

We can then bound the projection error

$$\begin{aligned} \|\Pi_{\mathcal{X}, d_{\mathcal{X}}}^n u - u\|_{L^p([-1, 1]^d)}^p &= \int_{[-1, 1]^d} |u - \tilde{u}|^p dx \\ &\leq C_d^p 2^d \|u\|_{C^s}^p r^{-ps} \\ &\leq C_d^p 2^d \|u\|_{C^s}^p d_{\mathcal{X}}^{-\frac{ps}{d}}. \end{aligned}$$

Therefore,

$$\|\Pi_{\mathcal{X}, d_{\mathcal{X}}}^n u - u\|_{L^p([-1, 1]^d)}^2 \leq C_d^2 2^{2d/p} \|u\|_{C^s}^2 d_{\mathcal{X}}^{-\frac{2s}{d}}.$$

Similarly, we can also derive that

$$\|\Pi_{\mathcal{Y}, d_{\mathcal{Y}}}^n(w) - w\|_{L^p([-1, 1]^d)}^2 \leq C_d^2 2^{2d/p} \|u\|_{C^s}^2 d_{\mathcal{X}}^{-\frac{2s}{d}} L_\Phi^2,$$

if the output function w has the same regularity as the input function u .

In the following, we present multiple PDE examples that satisfy Assumptions 2.10, Assumption 2.12, and Assumption 2.15, respectively. In particular, the solution operators of Poisson equation, parabolic equation, and transport equation are linear operators, implying that Assumption 2.12 is satisfied with g_i 's being the identity functions with $d_0 = 1$. The solution operator of Burgers equation is the composition of multiple numerical integration, the pointwise evaluation of an exponential function $g_j^1(\cdot) = \exp(\cdot)$, and the pointwise division $g_j^2(a, b) = a/b$. It thus satisfies Assumption 2.15 with $d_1 = 1$ and $d_2 = 2$. In parametric equations, we consider the forward operator that maps a media function $a(x)$ to the solution u . In most applications of such forward maps, the media function $a(x)$ represents natural images, such as CT scans for breast cancer diagnosis. Therefore, it is often assumed that Assumption 2.10 holds.

3.1 Poisson equation

For the following Poisson equation

$$\Delta u = f, \tag{3.1}$$

where $x \in \mathbb{R}^n$, and $|u(x)| \rightarrow 0$ as $|x| \rightarrow \infty$, the fundamental solution of (3.1) is given as

$$\Phi(x) = \begin{cases} \frac{1}{2\pi} \ln |x|, & \text{for } d = 2, \\ \frac{1}{w_n} |x|^{2-d}, & \text{for } d \geq 3. \end{cases}$$

Here w_n is the surface area of a unit ball in \mathbb{R}^d . Assume that the source $f(x)$ is a smooth function compactly supported in \mathbb{R}^d , then a unique solution to (3.1) can be given as follows

$$u(x) = (\Phi * f)(x) \begin{cases} \frac{1}{2\pi} \int_{\mathbb{R}^2} \ln |y| f(x-y) dy & \text{for } d = 2, \\ \frac{-1}{w_n} \int_{\mathbb{R}^d} |y|^{2-d} f(x-y) dy & \text{for } d \geq 3. \end{cases}$$

Notice that the solution map $f \mapsto u$ is a convolution with the fundamental solution, $u(x) = \Phi * f$. To show the solution operator is bounded, we assume the sources $f, g \in C^k(\mathbb{R}^d)$ and apply Young's inequality to get

$$\begin{aligned} \|u - v\|_{C^k(\Omega)} &= \|D^k(u - v)\|_{L^\infty(\Omega)} \\ &= \|\Phi * D^k(f - g)\|_{L^\infty(\Omega)} \\ &\leq \|\Phi\|_{L^p(\Omega)} \|f - g\|_{W^{k,q}(\Omega)} \\ &= \|\Phi\|_{L^p(\Omega)} \|f - g\|_{C^k(\mathbb{R}^d)} |\Omega|^{1/q}, \end{aligned} \tag{3.2}$$

where $p, q \geq 1$ so that $1/p + 1/q = 1$. Here Ω is any bounded domain.

For the Poisson equation on an unbounded domain (c.f. (3.1)), the computation is often implemented over a truncated finite domain Ω . For simplicity, we assume the source condition f is randomly generated in the space $C^k(\Omega)$. Since the solution u is a convolution of source f with a smooth kernel, both f and u are in $C^k(\Omega)$.

We then choose the encoder and decoder to be the spectral method. Applying Lemma 3.1, the encoder and decoder error of the input space can be calculated as the following:

$$\mathbb{E}_f \left[\|\Pi_{\mathcal{X}, d_{\mathcal{X}}}^n(f) - f\|_{L^2(\Omega)}^2 \right] \leq C_d d_{\mathcal{X}}^{-\frac{2k}{d}} \mathbb{E}_f \left[\|f\|_{C^k(\Omega)}^2 \right].$$

Similarly, applying Lemma 3.1 and (3.2), the encoder and decoder error of the output space is

$$\begin{aligned} &\mathbb{E}_{\mathcal{S}} \mathbb{E}_{f \sim \Phi_{\#} \gamma} \left[\|\Pi_{\mathcal{Y}, d_{\mathcal{Y}}}^n(u) - u\|_{L^2(\Omega)}^2 \right] \\ &= \mathbb{E}_f \left[\|\Pi_{\mathcal{Y}, d_{\mathcal{Y}}}^n(\Phi * f) - \Phi * f\|_{L^2(\Omega)}^2 \right] \\ &\leq C_d d_{\mathcal{Y}}^{-\frac{2k}{d}} \mathbb{E}_f \left[\|\Phi * f\|_{C^k(\Omega)}^2 \right] \\ &\leq C_d \|\Phi\|_{L^2(\Omega)}^2 |\Omega| d_{\mathcal{Y}}^{-\frac{2k}{d}} \mathbb{E}_f \left[\|f\|_{C^k(\Omega)}^2 \right]. \end{aligned}$$

By applying Theorem 2.13, we obtain that

$$\begin{aligned} &\mathbb{E}_{\mathcal{S}} \mathbb{E}_f \|D_{\mathcal{Y}}^n \circ \Gamma_{\text{NN}} \circ E_{\mathcal{X}}^n(f) - \Psi(f)\|_{L^2(\Omega)}^2 \\ &\lesssim d_{\mathcal{Y}}^{5/3} n^{-2/3} \log^6 n + (\sigma^2 + n^{-1}) \\ &\quad + r^{-2k} \mathbb{E}_f \left[\|f\|_{C^k(\Omega)}^2 \right], \end{aligned} \tag{3.3}$$

where the input dimension $d_{\mathcal{X}} = d_{\mathcal{Y}} = r^d$ and \lesssim contains constants that depend on $d_{\mathcal{X}}, d$ and $|\Omega|$.

Remark 3.2. If we can assume the solutions of interest lie on a low-dimensional manifold, the constants in (3.3) only depend on d, Ω and $\log d_{\mathcal{X}} = d \log r$, lessening the CoD since typically $d = 1, 2$, or 3 . Moreover, (3.3) suggests that the generalization error is small if we have a large number of samples, smaller noise, and good regularity of the input samples. Although the L^2 norm is used to bound the generalization error, the results can be generalized to any L^p norm with $1 < p < \infty$.

3.2 Parabolic equation

We consider the following parabolic equation

$$\begin{cases} u_t - \Delta u = 0 & \text{in } \mathbb{R}^d \times (0, \infty), \\ u = g & \text{on } \mathbb{R}^d \times \{t = 0\}. \end{cases} \tag{3.4}$$

The following function is the fundamental solution to (3.4):

$$\Phi(x, t) = \begin{cases} \frac{1}{(4\pi t)^{\frac{d}{2}}} e^{-\frac{|x|^2}{4t}}, & \text{for } x \in \mathbb{R}^d, t > 0, \\ 0, & \text{for } x \in \mathbb{R}^d, t < 0. \end{cases}$$

The solution map $g(\cdot) \mapsto u(T, \cdot)$ is a convolution with the fundamental solution: $u(\cdot, T) = \Phi(\cdot, T) * g$, where T is the terminal time. By Young's inequality, the Lipschitz constant is $\|\Phi(\cdot, T)\|_p$, where $1 \leq p \leq \infty$. As an example, we can explicitly calculate this number in 3D as $\|\Phi(\cdot, T)\|_p = p^{\frac{3}{2p}}$.

For the Parabolic equation (3.4), we assume a truncated finite computation domain $\Omega \times [0, T]$ and assume initial condition $g \in C^k(\Omega)$. Because the solution map has a similar convolution structure as in the Poisson equation, we can derive a similar result by Theorem 2.13

$$\begin{aligned} & \mathbb{E}_{\mathcal{S}} \mathbb{E}_g \|D_{\mathcal{Y}}^n \circ \Gamma_{\text{NN}} \circ E_{\mathcal{X}}^n(g) - \Psi(g)\|_{L^2(\Omega)}^2 \\ & \lesssim d_{\mathcal{Y}}^{5/3} n^{-2/3} \log^6 n \\ & + (\sigma^2 + n^{-1}) + r^{-2k} \mathbb{E}_g \left[\|g\|_{C^k(\Omega)}^2 \right]. \end{aligned} \quad (3.5)$$

Therefore, the CoD in parabolic equations is lessened according to (3.5) as in Poisson equations.

3.3 Transport equation

We consider the following transport equation,

$$\begin{cases} u_t + a(x) \cdot \nabla u = 0 & \text{in } \mathbb{R}^d \times (0, \infty), \\ u(0, x) = u_0(x) & \text{in } \mathbb{R}^d, \end{cases} \quad (3.6)$$

where $a(x)$ is the drift force field and $u_0(x)$ is the initial data. Here we assume that the drift force field satisfies

$$a \in C^2(\mathbb{R}^d) \cap W^{1, \infty}(\mathbb{R}^d)$$

for convenience. By the classical theory of ODE, the following initial value problem

$$\frac{dx(t)}{dt} = a(x(t)), \quad x(0) = x,$$

admits a unique solution for any $x \in \mathbb{R}^d$,

$$t \rightarrow x(t) = \varphi_t(x) \in C^1(\mathbb{R}; \mathbb{R}^d).$$

Note that for any $t \geq 0$, the vector valued function $\varphi_t : \mathbb{R}^d \rightarrow \mathbb{R}^d$ is a C^1 -diffeomorphism and

$$\mathbb{R}^+ \times \mathbb{R}^d \rightarrow \mathbb{R}^d, (t, x) \rightarrow \varphi_t(x)$$

is globally Lipschitz. Thanks to the Characteristic method, the solution of (3.6) is given by

$$u(t, x) := u_0(\varphi_t^{-1}(x)), \quad \text{for any } t \geq 0, x \in \mathbb{R}^d.$$

If we further assume that $u_0 \in H^s$ with $s > \frac{3d}{2}$, then by Theorem 5 of Section 7.3 of [44], we have $u \in C^1([0, \infty); \mathbb{R}^d)$. More specifically, we have

$$\|u(T, \cdot)\|_{C^1(\mathbb{R}^d)} \leq \|u_0\|_{H^s(\mathbb{R}^d)} C_{a, T, \Omega},$$

where $C_{a, T, \Omega} > 0$ is a constant that depends on the media a , terminal time T , and the support Ω of the initial data. Since the initial data has C^1 regularity, the encoder/decoder projection error of the input space is controlled via

$$\mathbb{E}_{u_0} \left[\|\Pi_{\mathcal{X}, d_{\mathcal{X}}}^n(u_0) - u_0\|_{L^2(\Omega)}^2 \right] \leq C_d d_{\mathcal{X}}^{-\frac{2}{d}} \mathbb{E}_f \left[\|u_0\|_{C^1(\Omega)}^2 \right].$$

Similarly, for the projection error of the output space, we have

$$\begin{aligned} & \mathbb{E}_{\mathcal{S}} \mathbb{E}_{u_0 \sim \Phi_{\#} \gamma} \left[\|\Pi_{\mathcal{Y}, d_{\mathcal{Y}}}^n(u) - u\|_{L^2(\Omega)}^2 \right] \\ & = \mathbb{E}_{u_0} \left[\|\Pi_{\mathcal{Y}, d_{\mathcal{Y}}}^n(u(T)) - u(T)\|_{L^2(\Omega)}^2 \right] \\ & \leq C_d d_{\mathcal{Y}}^{-\frac{2}{d}} \mathbb{E}_{u_0} \left[\|u(T)\|_{C^1(\Omega)}^2 \right] \\ & \leq C_{d, a, \Omega} d_{\mathcal{Y}}^{-\frac{2}{d}} \mathbb{E}_{u_0} \left[\|u_0\|_{H^s(\Omega)}^2 \right]. \end{aligned}$$

We then choose $d_{\mathcal{X}} = d_{\mathcal{Y}} = r^d$ and use Theorem 2.13 to derive that

$$\begin{aligned} & \mathbb{E}_{\mathcal{S}} \mathbb{E}_u \|D_{\mathcal{Y}}^n \circ \Gamma_{\text{NN}} \circ E_{\mathcal{X}}^n(u) - \Psi(u)\|_{L^2(\Omega)}^2 \\ & \leq d_{\mathcal{Y}}^{5/3} n^{-2/3} \log^6 n + (\sigma^2 + n^{-1}) \\ & + r^{-2} \mathbb{E}_g \left[\|u_0\|_{C^1(\Omega)}^2 + \|u_0\|_{H^s(\Omega)}^2 \right]. \end{aligned} \quad (3.7)$$

Therefore, the CoD in transport equations is lessened according to (3.7) as in other PDE examples.

3.4 Burgers equation

We consider the 1D Burgers equation with periodic boundary conditions:

$$\begin{cases} u_t + uu_x = \kappa u_{xx}, & \text{in } \mathbb{R} \times (0, \infty), \\ u(x, 0) = u_0(x), \\ u(-\pi, t) = u(\pi, t), \end{cases} \quad (3.8)$$

and we consider the solution map $u_0(\cdot) \mapsto u(T, \cdot)$. This solution map can be explicitly written using the Cole-Hopf transformation $u = \frac{-2\kappa v_x}{v}$ where

$$\begin{cases} v_t = \kappa v_{xx} \\ v(x, 0) = v_0(x) = \exp\left(-\frac{1}{2\kappa} \int_{-\pi}^x u_0(s) ds\right) \end{cases}$$

and the solution is given by

$$u(x, T) = -2\kappa \frac{\int_{\mathbb{R}} \partial_x \mathcal{K}(x, y, T) v_0(y) dy}{\int_{\mathbb{R}} \mathcal{K}(x, y, T) v_0(y) dy}$$

where the integration kernel \mathcal{K} is defined as $\mathcal{K}(x, y, t) = \frac{1}{\sqrt{4\pi\kappa t}} \exp\left(\frac{-(x-y)^2}{4\pi t}\right)$.

The solution of Burgers equation can be ill-posed in the sense that a shock will be formed in finite time for certain initial data, we have to assume that the terminal time T is small enough so that a shock is not formed yet. In fact, it is shown in [45] that if $T < c(1 + \|u_0\|_{H^s})^{-1}$ with $s > 3/2$, then

$$\|u(\cdot, T)\|_{H^s} \leq C \|u_0\|_{H^s}.$$

We further assume the regularity of initial data so that $\|u_0\|_{H^s}$ is finite. Then by Sobolev embedding, we have

$$\begin{aligned} \|u_0\|_{C^{k,\alpha}} &\leq C \|u_0\|_{H^s}, \\ \|u(\cdot, T)\|_{C^{k,\alpha}} &\leq C \|u_0\|_{H^s}, \end{aligned}$$

where $k + \alpha = s - 1/2$ and $0 < \alpha < 1$. By Lemma 3.1, we can control the encoder/decoder projection error for the initial data

$$\mathbb{E}_{u_0} \left[\|\Pi_{\mathcal{X}, d_{\mathcal{X}}}^n(u_0) - u_0\|_{L^2(\Omega)}^2 \right] \leq C_d d_{\mathcal{X}}^{-2s} \mathbb{E}_{u_0} [\|u_0\|_{H^s}^2],$$

and for the terminal solution

$$\begin{aligned} &\mathbb{E}_{u_0} \left[\|\Pi_{\mathcal{X}, d_{\mathcal{X}}}^n(u(\cdot, T)) - u(\cdot, T)\|_{L^2(\Omega)}^2 \right] \\ &\leq C d_{\mathcal{Y}}^{-2s} \mathbb{E}_{u_0} [\|u(\cdot, T)\|_{H^s}^2] \\ &\leq C d_{\mathcal{Y}}^{-2s} \mathbb{E}_{u_0} [\|u_0\|_{H^s}^2]. \end{aligned}$$

Similarly, we can choose $d_{\mathcal{X}} = d_{\mathcal{Y}} = r$ and use Theorem 2.16 to derive that

$$\begin{aligned} &\mathbb{E}_{\mathcal{S}} \mathbb{E}_u \|D_{\mathcal{Y}}^n \circ \Gamma_{\text{NN}} \circ E_{\mathcal{X}}^n(u(\cdot, T)) - \Psi(u(\cdot, T))\|_{L^2(\Omega)^2} \\ &\leq d_{\mathcal{Y}}^{3/2} n^{-1/2} \log^6 n + (\sigma^2 + n^{-1}) \\ &+ r^{-2s} \mathbb{E}_g [\|u_0\|_{H^s(\Omega)}^2]. \end{aligned} \quad (3.9)$$

Therefore, the CoD in Burgers equations is lessened according to (3.9) as in other PDE examples.

3.5 Parametric elliptic equation

We consider the 2D elliptic equation with heterogeneous media in this subsection.

$$\begin{cases} -\operatorname{div}(a(x)\nabla_x u(x)) = 0, & \text{in } \Omega \subset \mathbb{R}^2, \\ u = f, & \text{on } \partial\Omega. \end{cases} \quad (3.10)$$

The media coefficient $a(x)$ satisfies that $\alpha \leq a(x) \leq \beta$ for all $x \in \Omega$, where α and β are positive constants. We further assume that $a(x) \in C^1(\Omega)$. The solution is unique for any given boundary condition f so we can define the solution map:

$$S_a : f \in H^1 \mapsto u \in H^{3/2}.$$

We are interested in the forward map $a \mapsto u$, which has wide applications in inverse problems. Our goal is to compute the Frechét derivative $DS_a[\delta]$ with respect to a and derive an upper bound of the Lipschitz constant of the forward map. It can be shown that the Frechét derivative is

$$DS_a[\delta] : f \mapsto v_\delta,$$

where v_δ satisfies the following equation

$$\begin{cases} -\operatorname{div}(a(x)\nabla_x v_\delta(x)) = \operatorname{div}(\delta\nabla u), & \text{in } \Omega, \\ v_\delta = 0, & \text{on } \partial\Omega. \end{cases}$$

The above claim can be proved by using standard linearization argument and adjoint equation methods. Using classical elliptic regularity results, we derive that

$$\begin{aligned} \|v_\delta\|_{H^{3/2}} &\leq C\|\operatorname{div}(\delta\nabla u)\|_{H^{-1/2}} \\ &\leq C\|\delta\|_{L^\infty}\|u\|_{H^{3/2}} \leq C\|\delta\|_{L^\infty}\|f\|_{H^1}, \end{aligned}$$

where C only depends on the ambient dimension d and α, β . Therefore, the Lipschitz constant is $C\|f\|_{H^1}$. We apply Sobolev embedding and derive that $u \in C^{0,1/2}(\Omega)$. Since the parameter a has C^1 regularity, the encoder/decoder projection error of the input space is controlled

$$\mathbb{E}_a \left[\|\Pi_{\mathcal{X}, d_{\mathcal{X}}}^n(a) - a\|_{L^2(\Omega)}^2 \right] \leq C_d d_{\mathcal{X}}^{-1} \mathbb{E}_f \left[\|a\|_{C^1(\Omega)}^2 \right].$$

The solution only has $\frac{1}{2}$ Hölder regularity, so we have

$$\begin{aligned} &\mathbb{E}_{\mathcal{S}} \mathbb{E}_{a \sim \Phi_{\#} \gamma} \left[\|\Pi_{\mathcal{Y}, d_{\mathcal{Y}}}^n(u) - u\|_{L^2(\Omega)}^2 \right] \\ &= \mathbb{E}_a \left[\|\Pi_{\mathcal{Y}, d_{\mathcal{Y}}}^n(u) - \Phi * u\|_{L^2(\Omega)}^2 \right] \\ &\leq C d_{\mathcal{Y}}^{-\frac{1}{2}} \mathbb{E}_a \left[\|u\|_{C^{0,1/2}(\Omega)}^2 \right] \\ &\leq C_{\alpha, \beta, f} d_{\mathcal{Y}}^{-\frac{1}{2}}. \end{aligned}$$

Choosing $d_{\mathcal{X}} = d_{\mathcal{Y}} = r^2$ and applying Theorem 2.11, the generalization error is thus bounded by

$$\begin{aligned} &\mathbb{E}_{\mathcal{S}} \mathbb{E}_u \|D_{\mathcal{Y}}^n \circ \Gamma_{\text{NN}} \circ E_{\mathcal{X}}^n(u) - \Psi(u)\|_{L^2(\Omega)}^2 \\ &\leq d_{\mathcal{Y}}^{\frac{4+d_0}{2+d_0}} n^{-\frac{2}{2+d_0}} \log^6 n + (\sigma^2 + n^{-1}) \\ &\quad + r^{-2} \mathbb{E}_a \left[\|a\|_{C^1(\Omega)}^2 \right] + r^{-1} C_{\alpha, \beta, f}. \end{aligned}$$

Here d_0 is a constant that characterized the manifold dimension of the data set of media function $a(x)$ and, hence, the CoD of the parametric elliptic equations is mitigated.

4 Conclusion

To better understand the recent compelling experiment results of the DNN surrogate method for PDE problems, our work considers the fully connected DNNs for general PDE solution operators. We established an explicit training sample complexity estimate for the generalization error. When the solution of PDE lies in a low-dimensional manifold, or the solution space has low complexity, we found that the estimate can be improved to logarithmically depend on the resolution of the problem and thus lessening the CoD. Our result can be treated as a theoretical explanation of why the CoD of deep operator learning is lessened in PDE applications.

Acknowledgements

C. W. was partially supported by National Science Foundation Award DMS-2136380 and DMS-2206332. K.C. and H. Y. were partially supported by the US National Science Foundation under award DMS-2244988, DMS-2206333, and the Office of Naval Research Award N00014-23-1-2007. The authors thank Cheng Yu for the discussion of PDE solution operators in Section 3.

References

- [1] Benjamin Peherstorfer and Karen Willcox. Data-driven operator inference for nonintrusive projection-based model reduction. *Computer Methods in Applied Mechanics and Engineering*, 306:196–215, 2016.
- [2] Lu Lu, Pengzhan Jin, Guofei Pang, Zhongqiang Zhang, and George Em Karniadakis. Learning nonlinear operators via deepnet based on the universal approximation theorem of operators. *Nature Machine Intelligence*, 3(3):218–229, 2021.
- [3] Zongyi Li, Nikola Kovachki, Kamyar Azizzadenesheli, Burigede Liu, Kaushik Bhattacharya, Andrew Stuart, and Anima Anandkumar. Fourier neural operator for parametric partial differential equations. *arXiv preprint arXiv:2010.08895*, 2020.
- [4] Yuehaw Khoo and Lexing Ying. Switchnet: a neural network model for forward and inverse scattering problems. *SIAM Journal on Scientific Computing*, 41(5):A3182–A3201, 2019.
- [5] Mo Deng, Shuai Li, Alexandre Goy, Iksung Kang, and George Barbastathis. Learning to synthesize: robust phase retrieval at low photon counts. *Light: Science & Applications*, 9(1):1–16, 2020.
- [6] Chang Qiao, Di Li, Yuting Guo, Chong Liu, Tao Jiang, Qionghai Dai, and Dong Li. Evaluation and development of deep neural networks for image super-resolution in optical microscopy. *Nature Methods*, 18(2):194–202, 2021.
- [7] Chunwei Tian, Lunke Fei, Wenxian Zheng, Yong Xu, Wangmeng Zuo, and Chia-Wen Lin. Deep learning on image denoising: An overview. *Neural Networks*, 131:251–275, 2020.
- [8] Alex Graves, Abdel-rahman Mohamed, and Geoffrey Hinton. Speech recognition with deep recurrent neural networks. In *2013 IEEE international conference on acoustics, speech and signal processing*, pages 6645–6649. Ieee, 2013.
- [9] Riccardo Miotto, Fei Wang, Shuang Wang, Xiaoqian Jiang, and Joel T Dudley. Deep learning for healthcare: review, opportunities and challenges. *Briefings in bioinformatics*, 19(6):1236–1246, 2018.
- [10] Alex Krizhevsky, Ilya Sutskever, and Geoffrey E Hinton. Imagenet classification with deep convolutional neural networks. *Communications of the ACM*, 60(6):84–90, 2017.
- [11] Samuel Lanthaler, Siddhartha Mishra, and George E Karniadakis. Error estimates for deepnets: A deep learning framework in infinite dimensions. *Transactions of Mathematics and Its Applications*, 6(1):tnac001, 2022.
- [12] Nicholas H Nelsen and Andrew M Stuart. The random feature model for input-output maps between banach spaces. *SIAM Journal on Scientific Computing*, 43(5):A3212–A3243, 2021.
- [13] Chensen Lin, Zhen Li, Lu Lu, Shengze Cai, Martin Maxey, and George Em Karniadakis. Operator learning for predicting multiscale bubble growth dynamics. *The Journal of Chemical Physics*, 154(10):104118, 2021.
- [14] Shengze Cai, Zhicheng Wang, Lu Lu, Tamer A Zaki, and George Em Karniadakis. Deepm&net: Inferring the electroconvection multiphysics fields based on operator approximation by neural networks. *Journal of Computational Physics*, 436:110296, 2021.
- [15] Zongyi Li, Nikola Kovachki, Kamyar Azizzadenesheli, Burigede Liu, Kaushik Bhattacharya, Andrew Stuart, and Anima Anandkumar. Neural operator: Graph kernel network for partial differential equations. *arXiv preprint arXiv:2003.03485*, 2020.
- [16] Lu Lu, Xuhui Meng, Shengze Cai, Zhiping Mao, Somdatta Goswami, Zhongqiang Zhang, and George Em Karniadakis. A comprehensive and fair comparison of two neural operators (with practical extensions) based on fair data. *Computer Methods in Applied Mechanics and Engineering*, 393:114778, 2022.
- [17] Yong Zheng Ong, Zuowei Shen, and Haizhao Yang. Integral autoencoder network for discretization-invariant learning. *Journal of Machine Learning Research*, 23(286):1–45, 2022.
- [18] George Cybenko. Approximation by superpositions of a sigmoidal function. *Mathematics of control, signals and systems*, 2(4):303–314, 1989.
- [19] Kurt Hornik. Approximation capabilities of multilayer feedforward networks. *Neural networks*, 4(2):251–257, 1991.
- [20] Zuowei Shen, Haizhao Yang, and Shijun Zhang. Deep network approximation characterized by number of neurons. *arXiv preprint arXiv:1906.05497*, 2019.
- [21] Dmitry Yarotsky. Elementary superexpressive activations. In *International Conference on Machine Learning*, pages 11932–11940. PMLR, 2021.
- [22] Zuowei Shen, Haizhao Yang, and Shijun Zhang. Deep network with approximation error being reciprocal of width to power of square root of depth. *Neural Computation*, 33(4):1005–1036, 2021.

- [23] Dmitry Yarotsky. Optimal approximation of continuous functions by very deep relu networks. In *Conference on learning theory*, pages 639–649. PMLR, 2018.
- [24] Jianfeng Lu, Zuowei Shen, Haizhao Yang, and Shijun Zhang. Deep network approximation for smooth functions. *SIAM Journal on Mathematical Analysis*, 53(5):5465–5506, 2021.
- [25] Taiji Suzuki. Adaptivity of deep relu network for learning in besov and mixed smooth besov spaces: optimal rate and curse of dimensionality. *arXiv preprint arXiv:1810.08033*, 2018.
- [26] Andrew R Barron. Universal approximation bounds for superpositions of a sigmoidal function. *IEEE Transactions on Information theory*, 39(3):930–945, 1993.
- [27] Chao Ma, Lei Wu, et al. The barron space and the flow-induced function spaces for neural network models. *Constructive Approximation*, 55(1):369–406, 2022.
- [28] Nikola Kovachki, Samuel Lanthaler, and Siddhartha Mishra. On universal approximation and error bounds for fourier neural operators. *Journal of Machine Learning Research*, 22:Art–No, 2021.
- [29] Benedikt Bauer and Michael Kohler. On deep learning as a remedy for the curse of dimensionality in nonparametric regression. *The Annals of Statistics*, 47(4):2261–2285, 2019.
- [30] Minshuo Chen, Haoming Jiang, Wenjing Liao, and Tuo Zhao. Nonparametric regression on low-dimensional manifolds using deep relu networks: Function approximation and statistical recovery. *Information and Inference: A Journal of the IMA*, 11(4):1203–1253, 2022.
- [31] Max H Farrell, Tengyuan Liang, and Sanjog Misra. Deep neural networks for estimation and inference. *Econometrica*, 89(1):181–213, 2021.
- [32] Michael Kohler and Adam Krzyżak. Adaptive regression estimation with multilayer feedforward neural networks. *Nonparametric Statistics*, 17(8):891–913, 2005.
- [33] Hao Liu, Minshuo Chen, Tuo Zhao, and Wenjing Liao. Besov function approximation and binary classification on low-dimensional manifolds using convolutional residual networks. In *International Conference on Machine Learning*, pages 6770–6780. PMLR, 2021.
- [34] Ryumei Nakada and Masaaki Imaizumi. Adaptive approximation and generalization of deep neural network with intrinsic dimensionality. *J. Mach. Learn. Res.*, 21(174):1–38, 2020.
- [35] Johannes Schmidt-Hieber. Nonparametric regression using deep neural networks with relu activation function. *The Annals of Statistics*, 48(4):1875–1897, 2020.
- [36] Charles J Stone. Optimal global rates of convergence for nonparametric regression. *The annals of statistics*, pages 1040–1053, 1982.
- [37] Minshuo Chen, Haoming Jiang, Wenjing Liao, and Tuo Zhao. Efficient approximation of deep relu networks for functions on low dimensional manifolds. *Advances in neural information processing systems*, 32, 2019.
- [38] Alexander Cloninger and Timo Klock. Relu nets adapt to intrinsic dimensionality beyond the target domain. 2020.
- [39] Johannes Schmidt-Hieber. Deep relu network approximation of functions on a manifold. *arXiv preprint arXiv:1908.00695*, 2019.
- [40] Abdellah Chkifa, Albert Cohen, and Christoph Schwab. Breaking the curse of dimensionality in sparse polynomial approximation of parametric pdes. *Journal de Mathématiques Pures et Appliquées*, 103(2):400–428, 2015.
- [41] Maarten V de Hoop, Nikola B Kovachki, Nicholas H Nelsen, and Andrew M Stuart. Convergence rates for learning linear operators from noisy data. *arXiv preprint arXiv:2108.12515*, 2021.
- [42] Hao Liu, Haizhao Yang, Minshuo Chen, Tuo Zhao, and Wenjing Liao. Deep nonparametric estimation of operators between infinite dimensional spaces. *arXiv preprint arXiv:2201.00217*, 2022.
- [43] Partha Niyogi, Stephen Smale, and Shmuel Weinberger. Finding the homology of submanifolds with high confidence from random samples. *Discrete & Computational Geometry*, 39(1):419–441, 2008.
- [44] Lawrence C Evans. *Partial differential equations*, volume 19. American Mathematical Soc., 2010.
- [45] Nikolay Tzvetkov. Ill-posedness issues for nonlinear dispersive equations. *arXiv preprint math/0411455*, 2004.
- [46] Dmitry Yarotsky. Error bounds for approximations with deep relu networks. *Neural Networks*, 94:103–114, 2017.
- [47] Martin Anthony, Peter L Bartlett, Peter L Bartlett, et al. *Neural network learning: Theoretical foundations*, volume 9. cambridge university press Cambridge, 1999.
- [48] Peter L Bartlett, Nick Harvey, Christopher Liaw, and Abbas Mehrabian. Nearly-tight vc-dimension and pseudodimension bounds for piecewise linear neural networks. *The Journal of Machine Learning Research*, 20(1):2285–2301, 2019.

A Appendix

Proof of Theorem 2.7. The L^2 squared error can be decomposed as

$$\begin{aligned} & \mathbb{E}_{\mathcal{S}} \mathbb{E}_{u \sim \gamma} [\|D_{\mathcal{Y}}^n \circ \Gamma_{\text{NN}} \circ E_{\mathcal{X}}^n(u) - \Phi(u)\|_{\mathcal{Y}}^2] \\ & \leq 2\mathbb{E}_{\mathcal{S}} \mathbb{E}_{u \sim \gamma} [\|D_{\mathcal{Y}}^n \circ \Gamma_{\text{NN}} \circ E_{\mathcal{X}}^n(u) - D_{\mathcal{Y}}^n \circ E_{\mathcal{Y}}^n \circ \Phi(u)\|_{\mathcal{Y}}^2] + 2\mathbb{E}_{\mathcal{S}} \mathbb{E}_{u \sim \gamma} [\|D_{\mathcal{Y}}^n \circ E_{\mathcal{Y}}^n \circ \Phi(u) - \Phi(u)\|_{\mathcal{Y}}^2] \end{aligned}$$

where the first term $\text{I} = 2\mathbb{E}_{\mathcal{S}} \mathbb{E}_{u \sim \gamma} [\|D_{\mathcal{Y}}^n \circ \Gamma_{\text{NN}} \circ E_{\mathcal{X}}^n(u) - D_{\mathcal{Y}}^n \circ E_{\mathcal{Y}}^n \circ \Phi(u)\|_{\mathcal{Y}}^2]$ is the network estimation error in the \mathcal{Y} space, and $\text{II} = 2\mathbb{E}_{\mathcal{S}} \mathbb{E}_{u \sim \gamma} [\|D_{\mathcal{Y}}^n \circ E_{\mathcal{Y}}^n \circ \Phi(u) - \Phi(u)\|_{\mathcal{Y}}^2]$ is the empirical projection error, which can also be written as

$$\text{II} = 2\mathbb{E}_{\mathcal{S}} \mathbb{E}_{w \sim \Phi_{\#} \gamma} [\|\Pi_{\mathcal{Y}, d_{\mathcal{Y}}}^n(w) - w\|_{\mathcal{Y}}^2] \quad (\text{A.1})$$

We aim to derive an upper bound of I in the following. First, we notice that the decoder $D_{\mathcal{Y}}^n$ is Lipschitz, so that

$$\begin{aligned} \text{I} & = 2\mathbb{E}_{\mathcal{S}} \mathbb{E}_{u \sim \gamma} [\|D_{\mathcal{Y}}^n \circ \Gamma_{\text{NN}} \circ E_{\mathcal{X}}^n(u) - D_{\mathcal{Y}}^n \circ E_{\mathcal{Y}}^n \circ \Phi(u)\|_{\mathcal{Y}}^2] \\ & \leq 2L_{D_{\mathcal{Y}}^n}^2 \mathbb{E}_{\mathcal{S}} \mathbb{E}_{u \sim \gamma} [\|\Gamma_{\text{NN}} \circ E_{\mathcal{X}}^n(u) - E_{\mathcal{Y}}^n \circ \Phi(u)\|_{\mathcal{Y}}^2] \end{aligned}$$

Conditioned on the data set \mathcal{S}_1 , we can derive that

$$\begin{aligned} & \mathbb{E}_{\mathcal{S}_2} \mathbb{E}_{u \sim \gamma} [\|\Gamma_{\text{NN}} \circ E_{\mathcal{X}}^n(u) - E_{\mathcal{Y}}^n \circ \Phi(u)\|_{\mathcal{Y}}^2] \\ & = 2\mathbb{E}_{\mathcal{S}_2} \left[\frac{1}{n} \sum_{i=n+1}^{2n} \|\Gamma_{\text{NN}} \circ E_{\mathcal{X}}^n(u_i) - E_{\mathcal{Y}}^n \circ \Phi(u_i)\|_{\mathcal{Y}}^2 \right] \\ & \quad + \mathbb{E}_{\mathcal{S}_2} \mathbb{E}_{u \sim \gamma} [\|\Gamma_{\text{NN}} \circ E_{\mathcal{X}}^n(u) - E_{\mathcal{Y}}^n \circ \Phi(u)\|_{\mathcal{Y}}^2] - 2\mathbb{E}_{\mathcal{S}_2} \left[\frac{1}{n} \sum_{i=n+1}^{2n} \|\Gamma_{\text{NN}} \circ E_{\mathcal{X}}^n(u_i) - E_{\mathcal{Y}}^n \circ \Phi(u_i)\|_{\mathcal{Y}}^2 \right] \\ & = T_1 + T_2 \end{aligned} \quad (\text{A.2})$$

where the first term $T_1 = 2\mathbb{E}_{\mathcal{S}_2} \left[\frac{1}{n} \sum_{i=n+1}^{2n} \|\Gamma_{\text{NN}} \circ E_{\mathcal{X}}^n(u_i) - E_{\mathcal{Y}}^n \circ \Phi(u_i)\|_{\mathcal{Y}}^2 \right]$ contains the DNN approximation error and projection error in the \mathcal{X} space, where the second term $T_2 = \mathbb{E}_{\mathcal{S}_2} \mathbb{E}_{u \sim \gamma} [\|\Gamma_{\text{NN}} \circ E_{\mathcal{X}}^n(u) - E_{\mathcal{Y}}^n \circ \Phi(u)\|_{\mathcal{Y}}^2] - T_1$ captures the variance.

To obtain an upper bound of T_1 , we first notice that

$$T_1 \leq 2\mathbb{E}_{\mathcal{S}_2} \left[\frac{1}{n} \sum_{i=n+1}^{2n} \|\Gamma_{\text{NN}} \circ E_{\mathcal{X}}^n(u_i) - E_{\mathcal{Y}}^n(v_i)\|_{\mathcal{Y}}^2 \right] + 2\mathbb{E}_{\mathcal{S}_2} \left[\frac{1}{n} \sum_{i=n+1}^{2n} \|E_{\mathcal{Y}}^n \circ \Phi(u_i) - E_{\mathcal{Y}}^n(v_i)\|_{\mathcal{Y}}^2 \right]$$

Using the definition of Γ_{NN} , we have

$$T_1 \leq 2\mathbb{E}_{\mathcal{S}_2} \left[\inf_{\Gamma \in \mathcal{F}_{\text{NN}}} \frac{1}{n} \sum_{i=n+1}^{2n} \|\Gamma \circ E_{\mathcal{X}}^n(u_i) - E_{\mathcal{Y}}^n(v_i)\|_{\mathcal{Y}}^2 \right] + 2L_{E_{\mathcal{Y}}^n}^2 \mathbb{E}_{\mathcal{S}_2} \frac{1}{n} \sum_{i=n+1}^{2n} \|\varepsilon_i\|_{\mathcal{Y}}^2$$

Furthermore, we have

$$\begin{aligned} T_1 & \leq 4\mathbb{E}_{\mathcal{S}_2} \left[\inf_{\Gamma \in \mathcal{F}_{\text{NN}}} \frac{1}{n} \sum_{i=n+1}^{2n} \|\Gamma \circ E_{\mathcal{X}}^n(u_i) - E_{\mathcal{Y}}^n \circ \Phi(u_i)\|_{\mathcal{Y}}^2 \right] + 6L_{E_{\mathcal{Y}}^n}^2 \mathbb{E}_{\mathcal{S}_2} \frac{1}{n} \sum_{i=n+1}^{2n} \|\varepsilon_i\|_{\mathcal{Y}}^2 \\ & \leq 4 \inf_{\Gamma \in \mathcal{F}_{\text{NN}}} \mathbb{E}_{\mathcal{S}_2} \left[\frac{1}{n} \sum_{i=n+1}^{2n} \|\Gamma \circ E_{\mathcal{X}}^n(u_i) - E_{\mathcal{Y}}^n \circ \Phi(u_i)\|_{\mathcal{Y}}^2 \right] + 6L_{E_{\mathcal{Y}}^n}^2 \mathbb{E}_{\mathcal{S}_2} \frac{1}{n} \sum_{i=n+1}^{2n} \|\varepsilon_i\|_{\mathcal{Y}}^2 \\ & = 4 \inf_{\Gamma \in \mathcal{F}_{\text{NN}}} \mathbb{E}_u [\|\Gamma \circ E_{\mathcal{X}}^n(u) - E_{\mathcal{Y}}^n \circ \Phi(u)\|_{\mathcal{Y}}^2] + 6L_{E_{\mathcal{Y}}^n}^2 \mathbb{E}_{\mathcal{S}_2} \frac{1}{n} \sum_{i=n+1}^{2n} \|\varepsilon_i\|_{\mathcal{Y}}^2 \end{aligned} \quad (\text{A.3})$$

where the second inequality is derived by Fatou's lemma. To control the first term on the right-handside above, we apply the following lemma:

Lemma A.1. *For any function $f \in W^{n, \infty}([-1, 1]^d)$, and $\epsilon \in (0, 1)$, assume that $\|f\|_{W^{n, \infty}} \leq 1$, then there exists a function $\tilde{f} \in \mathcal{F}_{\text{NN}}(1, L, p, K, \kappa, M)$ such that*

$$\|\tilde{f} - f\|_{\infty} < \epsilon$$

if the parameters of \mathcal{F}_{NN} are chosen as

$$\begin{aligned} L &= \mathcal{O}((n+d) \ln \epsilon^{-1} + n^2 \ln d + d^2), \quad p = \mathcal{O}(d^{d+n} \epsilon^{-\frac{d}{n}} n^{-d} 2^{d^2/n}), \\ K &= \mathcal{O}(n^{2-d} d^{d+n+2} 2^{\frac{d^2}{n}} \epsilon^{-\frac{d}{n}} \ln \epsilon), \quad \kappa = \mathcal{O}(M^2), \quad M = \mathcal{O}(d+n) \end{aligned} \quad (\text{A.4})$$

where all constants hidden in $\mathcal{O}(\cdot)$ do not dependent on any parameters.

Proof. This is a direct consequence of proof of Theorem 1 in [46] for $F_{n,d}$. \square

Notice that each entry $h(\cdot)$ of Γ_n^d is a function supported on $[-B, B]^{d_{\mathcal{X}}}$ with Lipschitz constant M where $B = R_{\mathcal{X}} L_{E_{\mathcal{X}}}^n$ and $R = R_{\mathcal{Y}} L_{E_{\mathcal{Y}}} = R_{\mathcal{X}} L_{\Phi} L_{E_{\mathcal{Y}}}$, apply Theorem 1 of [46] to $\frac{1}{R} h(\frac{\cdot}{B})$, then we can find $\tilde{\Gamma}_d^n \in \mathcal{F}_{\text{NN}}$ such that

$$\|\tilde{\Gamma}_d^n - \Gamma_n^d\|_{\infty} \leq \varepsilon_1 \quad (\text{A.5})$$

with parameters of \mathcal{F}_{NN} chosen as

$$\begin{aligned} L &= \mathcal{O}(d_{\mathcal{X}} \ln \varepsilon_1^{-1} + d_{\mathcal{X}} \ln(BR) + d_{\mathcal{X}}^2), \quad p = \mathcal{O}(\varepsilon_1^{-d_{\mathcal{X}}} 2^{d_{\mathcal{X}}^2}), \\ K &= \mathcal{O}(pL), \quad \kappa = \mathcal{O}(M^2), \quad M = \mathcal{O}(d_{\mathcal{X}} BR), \end{aligned} \quad (\text{A.6})$$

where the constants in \mathcal{O} does not depend on any parameters.

Then we can develop an estimate of T_1 as the following.

$$\begin{aligned} & \inf_{\Gamma \in \mathcal{F}_{\text{NN}}} \mathbb{E}_u [\|\Gamma \circ E_{\mathcal{X}}^n(u) - E_{\mathcal{Y}}^n \circ \Phi(u)\|_{\mathcal{Y}}^2] \\ & \leq \mathbb{E}_u [\|\tilde{\Gamma}_d^n \circ E_{\mathcal{X}}^n(u) - E_{\mathcal{Y}}^n \circ \Phi(u)\|_{\mathcal{Y}}^2] \\ & \leq 2\mathbb{E}_u [\|\tilde{\Gamma}_d^n \circ E_{\mathcal{X}}^n(u) - \Gamma_d \circ E_{\mathcal{X}}^n(u)\|_{\mathcal{Y}}^2] + 2\mathbb{E}_u [\|\Gamma_d \circ E_{\mathcal{X}}^n(u) - E_{\mathcal{Y}}^n \circ \Phi(u)\|_{\mathcal{Y}}^2] \\ & \leq 2d_{\mathcal{Y}} \varepsilon_1^2 + 2\mathbb{E}_u [\|\Gamma_d \circ E_{\mathcal{X}}^n(u) - E_{\mathcal{Y}}^n \circ \Phi(u)\|_{\mathcal{Y}}^2]. \end{aligned} \quad (\text{A.7})$$

where the first inequality holds for the definition of infimum, the second for the triangle inequality, and the third from the approximation (A.5). Using the definition of Φ , we can derive further that

$$\begin{aligned} & \inf_{\Gamma \in \mathcal{F}_{\text{NN}}} \mathbb{E}_u [\|\Gamma \circ E_{\mathcal{X}}^n(u) - E_{\mathcal{Y}}^n \circ \Phi(u)\|_{\mathcal{Y}}^2] \\ & = 2d_{\mathcal{Y}} \varepsilon_1^2 + 2\mathbb{E}_u [\|E_{\mathcal{Y}}^n \circ \Phi \circ D_{\mathcal{X}}^n \circ E_{\mathcal{X}}^n(u) - E_{\mathcal{Y}}^n \circ \Phi(u)\|_{\mathcal{Y}}^2] \\ & \leq 2d_{\mathcal{Y}} \varepsilon_1^2 + 2L_{E_{\mathcal{Y}}}^2 L_{\Phi}^2 \mathbb{E}_u [\|D_{\mathcal{X}}^n \circ E_{\mathcal{X}}^n(u) - u\|_{\mathcal{Y}}^2] \\ & = 2d_{\mathcal{Y}} \varepsilon_1^2 + 2L_{E_{\mathcal{Y}}}^2 L_{\Phi}^2 \mathbb{E}_u [\|\Pi_{\mathcal{X}, d_{\mathcal{X}}}^n(u) - u\|_{\mathcal{Y}}^2], \end{aligned} \quad (\text{A.8})$$

where we used the Lipschitz continuity in the inequality. Combining (A.8) and (A.3), we have

$$T_1 \leq 8d_{\mathcal{Y}} \varepsilon_1^2 + 8L_{E_{\mathcal{Y}}}^2 L_{\Phi}^2 \mathbb{E}_u [\|\Pi_{\mathcal{X}, d_{\mathcal{X}}}^n(u) - u\|_{\mathcal{Y}}^2] + 6L_{E_{\mathcal{Y}}}^2 \tilde{\sigma}^2 \quad (\text{A.9})$$

To deal with the term T_2 , we have to use the covering number of \mathcal{F}_{NN} which has been done in lemma 6 and lemma 7 in [42]. A direct consequence of these two lemmas is

$$\begin{aligned} T_2 & \leq \frac{35d_{\mathcal{Y}} L_{E_{\mathcal{Y}}}^2 R_{E_{\mathcal{Y}}}^2}{n} \log \mathcal{N} \left(\frac{\delta}{4d_{\mathcal{Y}} L_{E_{\mathcal{Y}}}^n}, \mathcal{F}_{\text{NN}}, \|\cdot\|_{\infty} \right) + 6\delta \\ & \leq C \frac{d_{\mathcal{Y}}^2 K L_{E_{\mathcal{Y}}}^2 R_{E_{\mathcal{Y}}}^2}{n} (\ln \delta^{-1} + \ln L + \ln(pB) + L \ln \kappa + L \ln p) + C\delta \\ & \leq C \frac{d_{\mathcal{Y}}^2 K L_{E_{\mathcal{Y}}}^2 R_{E_{\mathcal{Y}}}^2}{n} (\ln \delta^{-1} + \ln(B) + L \ln \kappa + L \ln p) + C\delta \end{aligned}$$

where C is a universal constant and may change from line to line. We then choose parameters as shown in (A.6) and plug (A.6) into the above estimate, we have

$$\begin{aligned} T_2 & \leq C L_{E_{\mathcal{Y}}}^2 R_{E_{\mathcal{Y}}}^2 d_{\mathcal{Y}}^2 n^{-1} p L (\ln \delta^{-1} + L \ln B + L \ln R + L \ln p) + C\delta \\ & \leq C L_{E_{\mathcal{Y}}}^2 R_{E_{\mathcal{Y}}}^2 d_{\mathcal{Y}}^2 n^{-1} p L (\ln \delta^{-1} + L^2) + C\delta \\ & \leq C L_{E_{\mathcal{Y}}}^2 R_{E_{\mathcal{Y}}}^2 d_{\mathcal{Y}}^2 n^{-1} p (L^3 + (\ln \delta^{-1})^2) + C\delta \end{aligned}$$

where we have absorbed new absolute constants in C from line to line. We further plug in the values of p and L into the above estimate

$$\begin{aligned} T_2 &\leq CL_{E_y}^2 R_{E_y}^2 d_y^2 n^{-1} \varepsilon_1^{-d_x} 2^{d_x^2} (d_x^3 (\ln \varepsilon_1^{-1} + \ln(BR) + d_x)^3 + (\ln \delta^{-1})^2) + C\delta \\ &\leq CL_{E_y}^2 R_{E_y}^2 d_y^2 n^{-1} \varepsilon_1^{-d_x} 2^{d_x^2} ((\ln \varepsilon_1^{-1})^3 + (\ln(BR))^3 + (\ln \delta^{-1})^2) + C\delta \end{aligned}$$

Now we combine both the estimate above and the estimate for T_1 in (A.9),

$$\begin{aligned} T_1 + T_2 &\lesssim d_y \varepsilon_1^2 + L_{E_y}^2 R_{E_y}^2 d_y^2 n^{-1} \varepsilon_1^{-d_x} 2^{d_x^2} ((\ln \varepsilon_1^{-1})^3 + (\ln(BR))^3 + (\ln \delta^{-1})^2) \\ &\quad + L_{E_y}^2 L_{\Phi}^2 \mathbb{E}_u [\|\Pi_{\mathcal{X}, d_x}^n(u) - u\|_y^2] + L_{E_y}^2 \tilde{\sigma}^2 + \delta \end{aligned}$$

We aim to balance the above error and choose

$$\delta = n^{-1}, \quad \varepsilon_1 = d_y^{\frac{1}{2+d_x}} n^{-\frac{1}{2+d_x}}$$

Therefore,

$$\begin{aligned} T_1 + T_2 &\lesssim d_y^{\frac{4+d_x}{2+d_x}} n^{-\frac{2}{2+d_x}} L_{E_y}^2 R_{E_y}^2 2^{d_x^2} \left((\ln \frac{n}{d_y})^3 + (\ln(BR))^3 + (\ln n)^2 \right) \\ &\quad + L_{E_y}^2 L_{\Phi}^2 \mathbb{E}_u [\|\Pi_{\mathcal{X}, d_x}^n(u) - u\|_y^2] + L_{E_y}^2 \tilde{\sigma}^2 + n^{-1} \end{aligned} \tag{A.10}$$

with parameters chosen as

$$\begin{aligned} L &= \mathcal{O}(d_x \ln(\frac{n}{d_y}) + d_x \ln(BR) + d_x^2), \quad p = \mathcal{O}(d_y^{-\frac{d_x}{2+d_x}} n^{\frac{d_x}{2+d_x}} 2^{d_x^2}), \\ K &= \mathcal{O}(pL), \quad \kappa = \mathcal{O}(M^2), \quad M = \mathcal{O}(d_x BR), \end{aligned}$$

Combining (A.1) and (A.10) together, we have

$$\begin{aligned} \mathbb{E}_{\mathcal{S}} \mathbb{E}_{u \sim \gamma} [\|D_y^n \circ \Gamma_{\text{NN}} \circ E_{\mathcal{X}}^n(u) - \Phi(u)\|_y^2] &\lesssim d_y^{\frac{4+d_x}{2+d_x}} n^{-\frac{2}{2+d_x}} L_{E_y}^2 R_{E_y}^2 2^{d_x^2} \left((\ln \frac{n}{d_y})^3 + (\ln(BR))^3 + (\ln n)^2 \right) \\ &\quad + L_{E_y}^2 L_{\Phi}^2 \mathbb{E}_u [\|\Pi_{\mathcal{X}, d_x}^n(u) - u\|_y^2] + \mathbb{E}_{\mathcal{S}} \mathbb{E}_{w \sim \Phi \# \gamma} [\|\Pi_{\mathcal{Y}, d_y}^n(w) - w\|_y^2] \\ &\quad + L_{E_y}^2 \tilde{\sigma}^2 + n^{-1} \end{aligned}$$

□

Proof of Theorem 2.8. Similarly to the proof of Theorem 1, we have

$$\mathbb{E}_{\mathcal{S}} \mathbb{E}_u \|D_y^n \circ \Gamma_{\text{NN}} \circ E_{\mathcal{X}}^n(u) - \Psi(u)\|_y^2 \leq \text{I} + \text{II}$$

and

$$\text{I} \leq 2L_{D_y}^2 (T_1 + T_2)$$

where T_1 and T_2 are defined in (A.2). Following the same procedure in (A.3), we have

$$T_1 \leq 4 \inf_{\Gamma \in \mathcal{F}_{\text{NN}}} \mathbb{E}_u [\|\Gamma \circ E_{\mathcal{X}}^n(u) - E_y^n \circ \Phi(u)\|_y^2] + 6\mathbb{E}_{\mathcal{S}_2} \frac{1}{n} \sum_{i=n+1}^{2n} \|\varepsilon_i\|_y^2.$$

Under the new network architecture $\mathcal{F}_{\text{NN}}(d_y, L, p, M)$, we apply Theorem 1.1 in [20] so that for any $\varepsilon_1 > 0$, we can choose $\tilde{\Gamma}_d^n$ in \mathcal{F}_{NN} such that $\|\tilde{\Gamma}_d^n - \Gamma_d^n\|_{\infty} \leq CL_{\Phi} \varepsilon_1$ with suitable parameters choice

$$L = O(\tilde{L}), p = O(\tilde{p}), M = \sqrt{d_y} L_{E_y} R_y, \tag{A.11}$$

where $\tilde{L}, \tilde{p} > 0$ are integers such that $\tilde{L}\tilde{p} = \lceil \varepsilon_1^{-d_x/2} \rceil$. The constant hidden in C and $O(\cdot)$ depends on d_x . Similarly to that in Equation (A.7), we can derive that

$$T_1 \leq CL_{\Phi}^2 d_y \varepsilon_1^2 + 8L_{E_y}^2 L_{\Phi}^2 \mathbb{E}_u [\|\Pi_{\mathcal{X}, d_x}^n(u) - u\|_y^2] + 6\sigma^2 \tag{A.12}$$

To deal with term T_2 , we apply the following lemma concerning the covering number.

Lemma A.2. [Lemma 10 in [42]] Under the conditions of Theorem 2, we have

$$\mathbb{T}_2 \leq \frac{35d_{\mathcal{Y}}R_{\mathcal{Y}}^2}{n} \log \mathcal{N} \left(\frac{\delta}{4d_{\mathcal{Y}}L_{E_{\mathcal{Y}}}R_{\mathcal{Y}}}, \mathcal{F}_{\text{NN}}, 2n \right) + 6\delta.$$

Combining Lemma A.2 with (A.12), we derive that

$$\begin{aligned} \mathbb{I} &\leq CL_{\Phi}^2 L_{D_{\mathcal{Y}}}^2 d_{\mathcal{Y}} \varepsilon_1^2 + 16L_{D_{\mathcal{Y}}}^2 L_{E_{\mathcal{Y}}}^2 L_{\Phi}^2 \mathbb{E}_u [\|\Pi_{\mathcal{X}, d_{\mathcal{X}}}^n(u) - u\|_{\mathcal{Y}}^2] + 12L_{D_{\mathcal{Y}}}^2 \sigma^2 \\ &\quad + \frac{70L_{D_{\mathcal{Y}}}^2 d_{\mathcal{Y}} R_{\mathcal{Y}}^2}{n} \log \mathcal{N} \left(\frac{\delta}{4d_{\mathcal{Y}}L_{E_{\mathcal{Y}}}R_{\mathcal{Y}}}, \mathcal{F}_{\text{NN}}(d_{\mathcal{Y}}, L, p, M), 2n \right) + 12L_{D_{\mathcal{Y}}}^2 \delta \end{aligned} \quad (\text{A.13})$$

By the definition of covering number (c.f. Definition 5 in [42]), we first notice that the covering number of $\mathcal{F}_{\text{NN}}(d_{\mathcal{Y}}, L, p, M)$ is bounded by that of $\mathcal{F}_{\text{NN}}(1, L, p, M)$

$$\mathcal{N} \left(\frac{\delta}{4d_{\mathcal{Y}}L_{E_{\mathcal{Y}}}R_{\mathcal{Y}}}, \mathcal{F}_{\text{NN}}(d_{\mathcal{Y}}, L, p, M), 2n \right) \leq Ce^{d_{\mathcal{Y}}} \mathcal{N} \left(\frac{\delta}{4d_{\mathcal{Y}}L_{E_{\mathcal{Y}}}R_{\mathcal{Y}}}, \mathcal{F}_{\text{NN}}(1, L, p, M), 2n \right)$$

So it suffices to find an estimate on the covering number of $\mathcal{F}_{\text{NN}}(1, L, p, M)$. A generic bound for classes of functions is provided by the following lemma.

Lemma A.3 (Theorem 12.2 of [47]). *Let F be a class of functions from some domain Ω to $[-M, M]$. Denote the pseudo-dimension of F by $\text{Pdim}(F)$. For any $\delta > 0$, we have*

$$\mathcal{N}(\delta, F, m) \leq \left(\frac{2eMm}{\delta \text{Pdim}(F)} \right)^{\text{Pdim}(F)} \quad (\text{A.14})$$

for $m > \text{Pdim}(F)$.

The next lemma shows that for a DNN $\mathcal{F}_{\text{NN}}(1, L, p, M)$, its pseudo-dimension can be bounded by the network parameters.

Lemma A.4 (Theorem 7 of [48]). *For any network architecture \mathcal{F}_{NN} with L layers and U parameters, there exists a universal constant C such that*

$$\text{Pdim}(\mathcal{F}_{\text{NN}}) \leq CLU \log(U). \quad (\text{A.15})$$

Considering the network architecture $\mathcal{F}_{\text{NN}}(1, L, p, M)$, whose number of parameters is bounded by $U = Lp^2$, we can apply Lemma A.3 and A.4 to bound the covering number by its parameters.

$$\log \mathcal{N} \left(\frac{\delta}{4d_{\mathcal{Y}}L_{E_{\mathcal{Y}}}R_{\mathcal{Y}}}, \mathcal{F}_{\text{NN}}(d_{\mathcal{Y}}, L, p, M), 2n \right) \leq C_8 d_{\mathcal{Y}} p^2 L^2 \log(p^2 L) (\log M + \log \delta^{-1} + \log n) \quad (\text{A.16})$$

when $2n > C_9 p^2 L^2 \log(p^2 L)$ for some universal constant C_8, C_9 . Notice that the choice of p, L in (A.11) and $\tilde{L}\tilde{p} = \lceil \varepsilon_1^{-d_{\mathcal{X}}/2} \rceil$, we have

$$pL \leq \mathcal{O}(\tilde{p}\tilde{L} \log \tilde{L} \log \tilde{p}) \leq \mathcal{O}(\tilde{p}\tilde{L}(\log(\tilde{p}\tilde{L}))^2) \leq \mathcal{O}(d_{\mathcal{X}}^2 \varepsilon_1^{-d_{\mathcal{X}}/2} \log^2 \varepsilon_1^{-1}) \quad (\text{A.17a})$$

$$\log(pL) = \mathcal{O}(\log d_{\mathcal{X}} + d_{\mathcal{X}} \log \varepsilon_1^{-1} + \log \log \varepsilon_1^{-1}) = \mathcal{O}(d_{\mathcal{X}} \log \varepsilon_1^{-1}) \quad (\text{A.17b})$$

Substituting (A.17) into (A.16) gives rise to

$$\log \mathcal{N} \left(\frac{\delta}{4d_{\mathcal{Y}}L_{E_{\mathcal{Y}}}R_{\mathcal{Y}}}, \mathcal{F}_{\text{NN}}, 2n \right) \leq C_8 d_{\mathcal{Y}} d_{\mathcal{X}}^5 \varepsilon_1^{-d_{\mathcal{X}}} \log^5(\varepsilon_1^{-1}) (\log d_{\mathcal{Y}} + \log \delta^{-1} + \log n). \quad (\text{A.18})$$

where the constant C_8 may depend on $L_{E_{\mathcal{Y}}}$ and $R_{\mathcal{Y}}$. We then substitute the above covering number estimate back to (A.13),

$$\begin{aligned} \mathbb{I} &\leq CL_{\Phi}^2 L_{D_{\mathcal{Y}}}^2 d_{\mathcal{Y}} \varepsilon_1^2 + 16L_{D_{\mathcal{Y}}}^2 L_{E_{\mathcal{Y}}}^2 L_{\Phi}^2 \mathbb{E}_u [\|\Pi_{\mathcal{X}, d_{\mathcal{X}}}^n(u) - u\|_{\mathcal{Y}}^2] + 12L_{D_{\mathcal{Y}}}^2 \sigma^2 \\ &\quad + C_8 d_{\mathcal{Y}}^2 \varepsilon_1^{-d_{\mathcal{X}}} \log^5(\varepsilon_1^{-1}) (\log d_{\mathcal{Y}} + \log \delta^{-1} + \log n) n^{-1} + 12L_{D_{\mathcal{Y}}}^2 \delta \end{aligned}$$

where the constant C_8 may depend on $L_{E_{\mathcal{Y}}^n}, R_{\mathcal{Y}}, L_{D_{\mathcal{Y}}^n}, R_{\mathcal{Y}}$ and $d_{\mathcal{X}}$. Setting

$$\varepsilon_1 = d_{\mathcal{Y}}^{\frac{1}{2+d_{\mathcal{X}}}} n^{-\frac{1}{2+d_{\mathcal{X}}}}, \delta = n^{-1},$$

we have

$$\begin{aligned} \text{I} &\lesssim L_{\Phi}^2 d_{\mathcal{Y}}^{\frac{4+d_{\mathcal{X}}}{2+d_{\mathcal{X}}}} n^{-\frac{2}{2+d_{\mathcal{X}}}} + L_{\Phi}^2 \mathbb{E}_u [\|\Pi_{\mathcal{X}, d_{\mathcal{X}}}^n(u) - u\|_{\mathcal{Y}}^2] + (\sigma^2 + \delta) \\ &\quad + d_{\mathcal{Y}}^{\frac{4+d_{\mathcal{X}}}{2+d_{\mathcal{X}}}} n^{-\frac{2}{2+d_{\mathcal{X}}}} \log^6(n) L_{\Phi}^2 \\ &\lesssim L_{\Phi}^2 d_{\mathcal{Y}}^{\frac{4+d_{\mathcal{X}}}{2+d_{\mathcal{X}}}} n^{-\frac{2}{2+d_{\mathcal{X}}}} \log^6 n + (\sigma^2 + n^{-1}) + L_{\Phi}^2 \mathbb{E}_u [\|\Pi_{\mathcal{X}, d_{\mathcal{X}}}^n(u) - u\|_{\mathcal{Y}}^2] \end{aligned} \quad (\text{A.19})$$

where \lesssim contains constants that depend on $d_{\mathcal{X}}, L_{E_{\mathcal{Y}}^n}$ and $L_{D_{\mathcal{Y}}^n}$. Now combining our estimate (A.19) and (A.1), we have

$$\begin{aligned} \mathbb{E}_{\mathcal{S}} \mathbb{E}_u \|D_{\mathcal{Y}}^n \circ \Gamma_{\text{NN}} \circ E_{\mathcal{X}}^n(u) - \Psi(u)\|_{\mathcal{Y}}^2 &\lesssim L_{\Phi}^2 d_{\mathcal{Y}}^{\frac{4+d_{\mathcal{X}}}{2+d_{\mathcal{X}}}} n^{-\frac{2}{2+d_{\mathcal{X}}}} \log^6 n + (\sigma^2 + n^{-1}) \\ &\quad + L_{\Phi}^2 \mathbb{E}_u [\|\Pi_{\mathcal{X}, d_{\mathcal{X}}}^n(u) - u\|_{\mathcal{Y}}^2] + \mathbb{E}_{\mathcal{S}} \mathbb{E}_{w \sim \Phi_{\# \gamma}} [\|\Pi_{\mathcal{Y}, d_{\mathcal{Y}}}^n(w) - w\|_{\mathcal{Y}}^2] \end{aligned}$$

□

Proof of Theorem 2.11. The proof of Theorem 2.11 can be similarly done to that of Theorem 4 in [42] with the following changes. Instead of approximating the function $f := E_{\mathcal{Y}} \circ \Psi \circ D_{\mathcal{X}}$, we approximate $f_0(x) := \frac{f(x)}{L_{\Psi}}$ by a FNN architecture $\tilde{f}_0(x)$ and then modify the FNN by multiplying the constant L_{Ψ} so that $f(x) \approx L_{\Psi} \tilde{f}_0(x)$. This process will eliminate the constant dependence on L_{Ψ} of all intermediate theorems including Lemma 17 in [42]. □

Proof of Theorem 2.13. The proof is similar to that of Theorem 2.11. The first layer of Γ_{NN} consists of linear transforms $V_1, \dots, V_{d_{\mathcal{Y}}}$ while other layers will be used to learn nonlinear functions $g_k : \mathbb{R}^{d_0} \rightarrow \mathbb{R}, k = 1, \dots, d_{\mathcal{Y}}$. The DNN approximation of functions $g_k, k = 1, \dots, d_{\mathcal{Y}}$ is similar to that of functions on d_0 -dimensional manifold. □

Proof of Theorem 2.16. The proof is similar to that of Theorem 2.13. In particular, the whole DNN contains compositions of single linear layers and nonlinear layers that approximate $G^i : \mathbb{R}^{l_{i-1}} \rightarrow \mathbb{R}^{l_i}$. The DNN approximation to G^i 's is the same as that of the function g in the proof of Theorem 2.13. In particular, for each function G^i , its DNN would have parameter choice $L_i p_i = \varepsilon^{-d_i/2}$, where L_i is the number of layers and p_i is the number of parameters in each layer. □